The Precision Proton Spectrometer of CMS: Recent results and prospects

A. Solano on behalf of the CMS and TOTEM Collaborations

Università di Torino and INFN

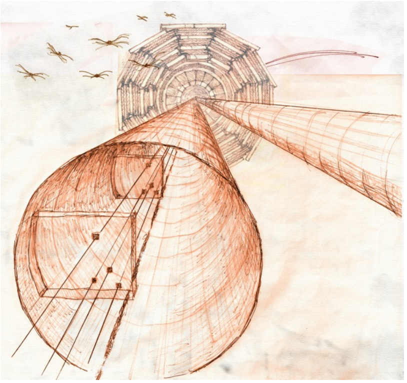

Diffraction & Low-x 2024

10/9/2024

Outline

- Project overview
- Detector performance
- Physics with proton tagging at 13 TeV
- Prospects – HL-LHC

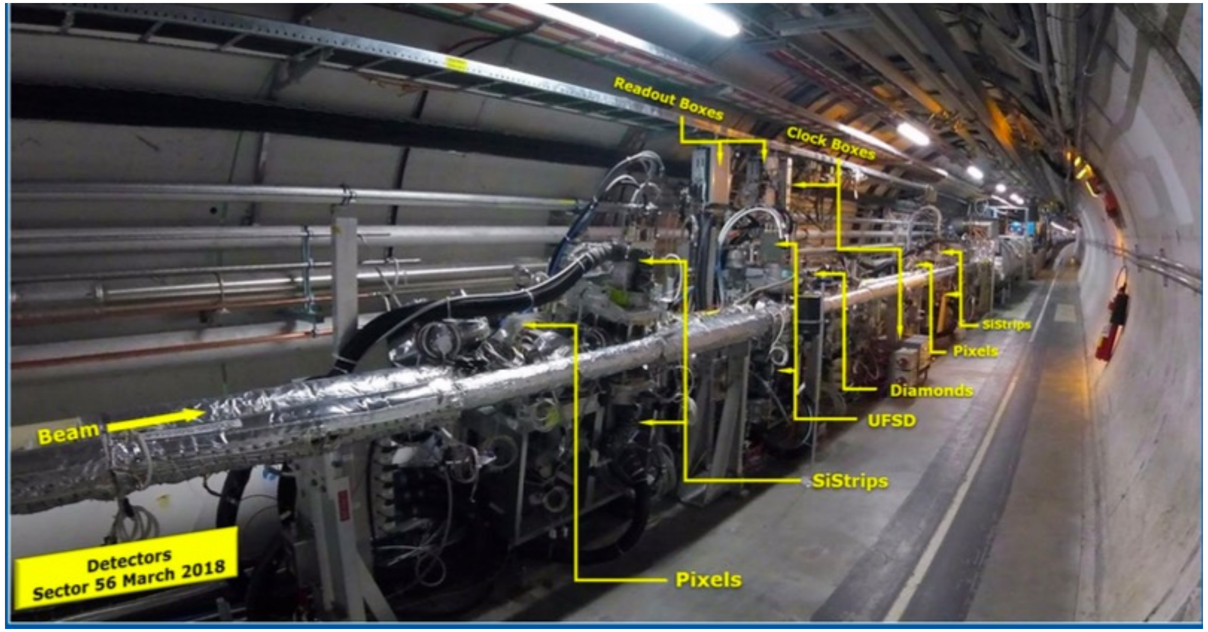

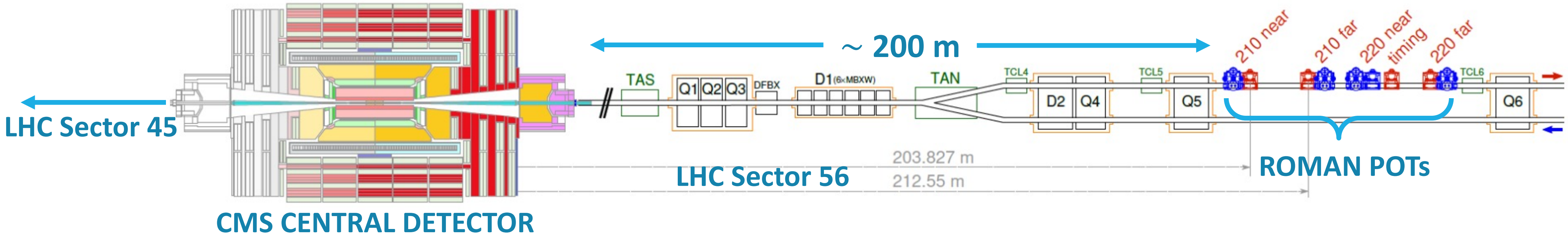

The CT-PPS - now PPS - project

The CMS-TOTEM Precision Proton Spectrometer (CT-PPS) has been **designed for measuring the scattered protons** on both sides of CMS **in standard LHC running conditions**, using LHC magnets to measure the proton momentum [TDR CERN-LHCC-2014-021].
Since April 2018, CT-PPS is a standard component of CMS, with name PPS.

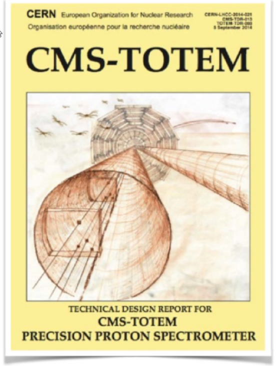

The PPS physics program focuses on Central Exclusive Production (CEP) processes of the type:

pp –> p X p with X = ll, high-E_T jets, WW, ZZ, $\gamma\gamma$, … $M_X = \sqrt{s\xi_1\xi_2}$

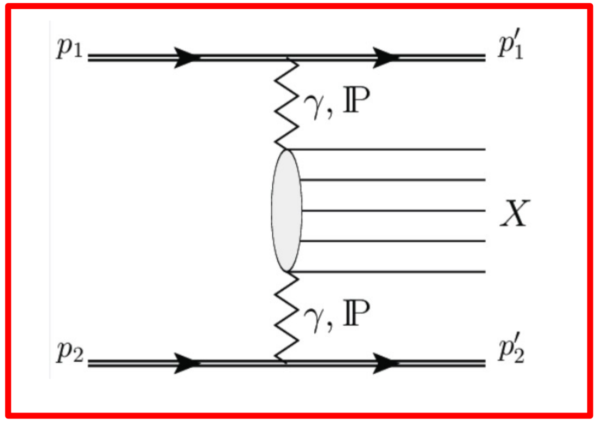

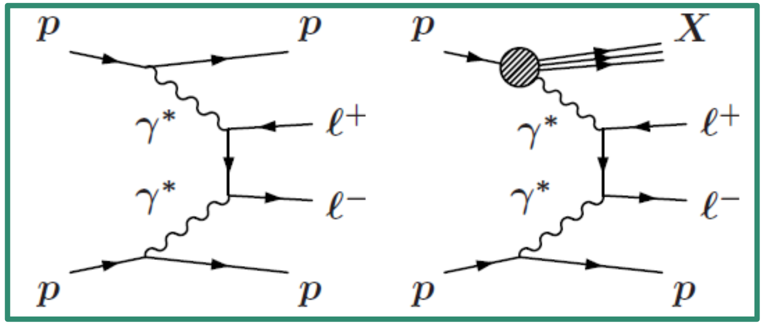

PPS first publication, JHEP07 (2018) 153

- **Tracking detectors** measure the proton displacement w.r.t. the beam, which is translated into the **proton fractional momentum loss (ξ)** thanks to the knowledge of the beam optics
- **Timing detectors** are used to disentangle pileup
- All are located inside Roman Pots so that they can be moved very close to the circulating beams

Experimental challenge and apparatus

- **Roman Pots need to operate at few mm from the beam (~1.5 mm) to maximize acceptance**
  -> Detectors must tolerate high levels of non-uniform irradiation
  - Proton fluence up to ~ 5×10^{15} protons/cm^2 for 100 fb^{-1} (Run2)
    Dose: ~ 1.61 Mrad/fb^{-1}
- **Spatial resolution goal:** ~ 10-30 μm
- **Timing resolution goal:** ~ 20-30 ps

Tracking detectors

Timing detectors

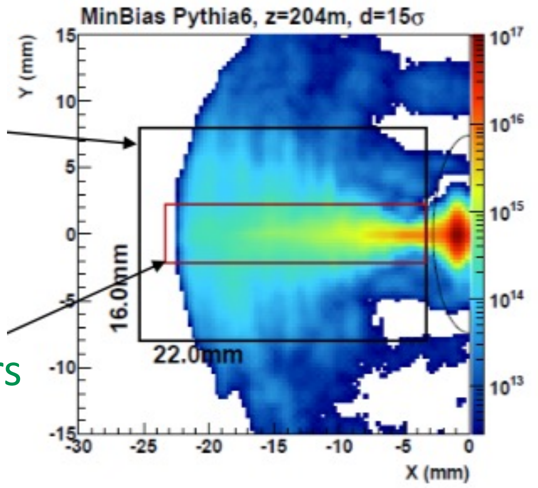

Data taking with different detector configurations in different years:

Very stable operation in both Run 2 and Run 3

Run 2:

2015	2016	2017	2018	2022 –>
Exploratory phase	**Strips + Diamonds**	**Strips + 3D Pixels + Diamonds + UFSD**	**3D Pixels + Single & double diamonds**	**Run 3: 3D Pixels + double diamonds**
Data recorded with tracking RPs inserted:	**L_{INT}~15 fb^{-1}** 39% OF THE DATA RECORDED BY CMS	**L_{INT}~40 fb^{-1}** 88% OF THE DATA RECORDED BY CMS	**L_{INT}~60 fb^{-1}** 93% OF THE DATA RECORDED BY CMS	**L_{INT} > 100 fb^{-1}** ~80% OF THE DATA RECORDED BY CMS

PPS integrated luminosity in Run 2: ~ 115 fb^{-1}

PPS integrated luminosity in Run 3 up to now: ~ 100 fb^{-1}

Detectors performance in 2023

Preliminary look at collected data

Tracker:

- Known inefficiency in the region closest to the beam, caused by the non-uniform irradiation of the ROC, mitigated by the **internal movement system of the detectors in the pot implemented for Run 3**
- Overall **optimal efficiency: > 98% average** on the full detector area

CMS DP-2024/008

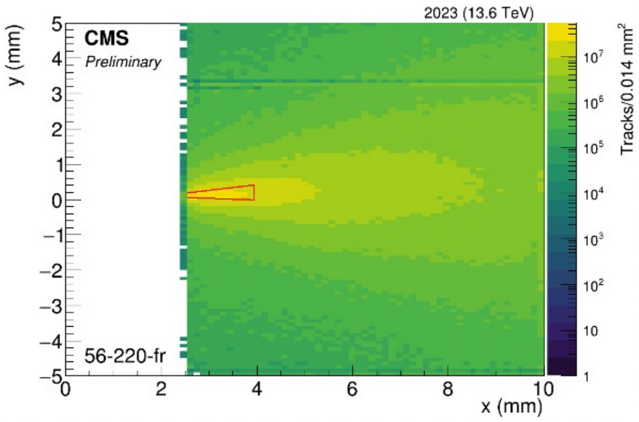

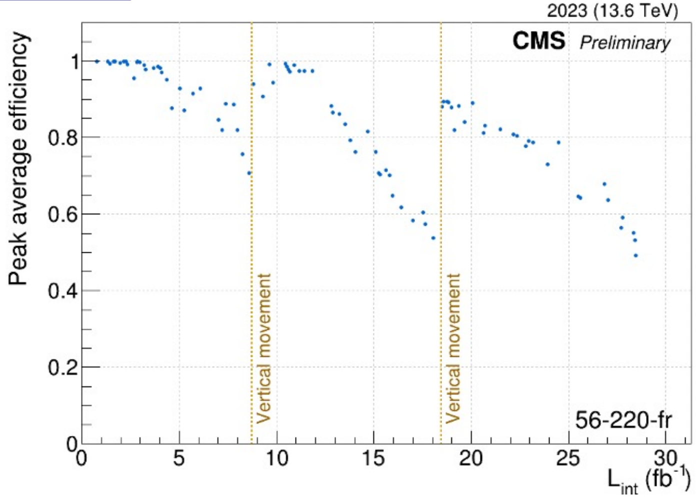

Timing detectors:

- Low-PU (<μ>=1) zero-bias data used to correlate PPS vertex from timing with CMS one:

$$z_{PPS,timing} - z_{vertex} = (c/2 \cdot \Delta t) - z_{vertex}$$

- Good correlation between Δt and z_{vertex}
- **1.9 cm vertex resolution** w.r.t. Run 2 measurement of 2.77 cm

CMS DP-2024/009

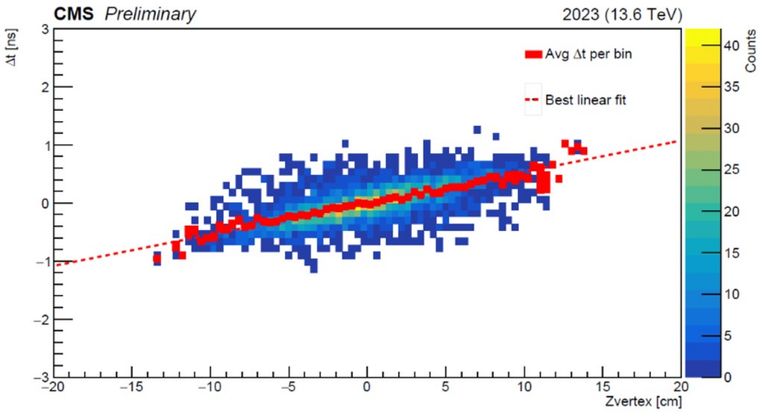

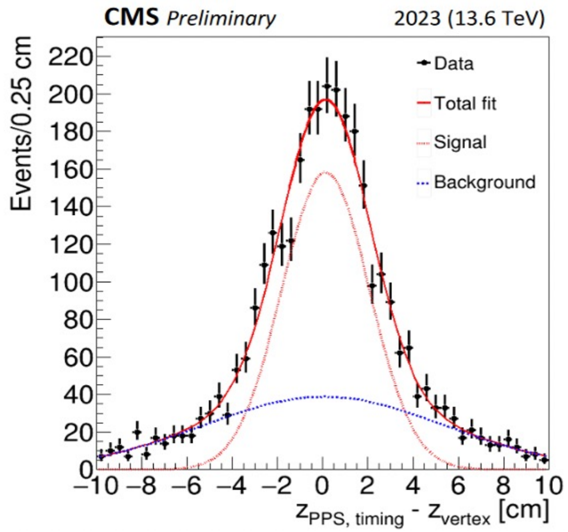

Proton reconstruction

The **proton reconstruction relies on**:

JINST 18 (2023) P09009

- the **alignment** of the detectors planes w.r.t. the LHC beam
- the knowledge of the transport matrices parametrising the LHC magnet lattice, referred to as **beam optics**

Reconstructed hits in PPS tracker → proton **tracks** → **proton kinematics** at the IP

Local alignment, done once among detectors in each pot

Global alignment with beam, done for each physics fill

LHC lattice knowledge + optics calibration with data

Detector alignment:

Multi-step procedure with base measurement in dedicated LHC fill

Alignment run:

- Low intensity, detectors closer to the beam + vertical RPs in
- Elastic scattering kinematic properties used to find the beam centre

The **proton kinematics at the IP** are obtained from the measured track positions at the RPs by **back-propagating the proton from the RPs to the IP according to the LHC optics:**

$$x = v_x(\xi) \cdot x^* + L_x(\xi) \cdot \theta_x^* + D_x(\xi) \cdot \xi$$

$$y = v_y(\xi) \cdot y^* + L_y(\xi) \cdot \theta_y^* + D_y(\xi) \cdot \xi$$

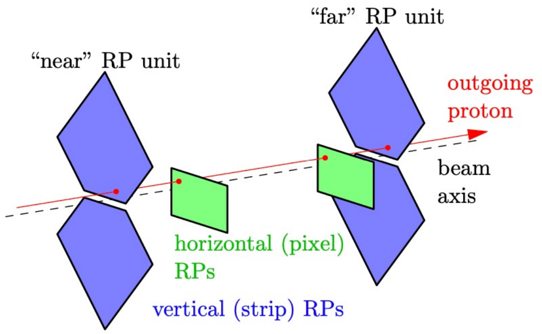

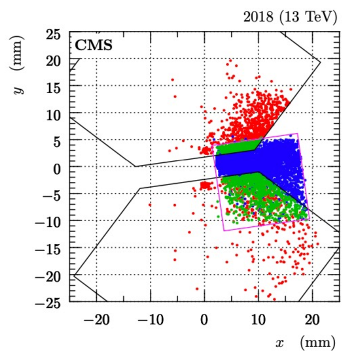

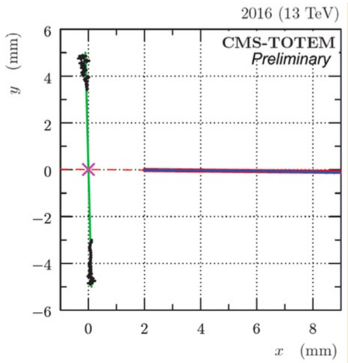

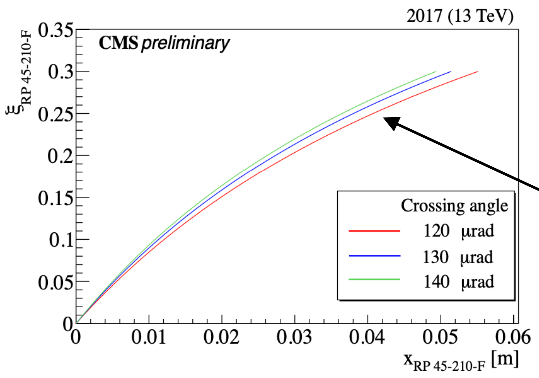

Di-lepton exclusive production as a validation tool

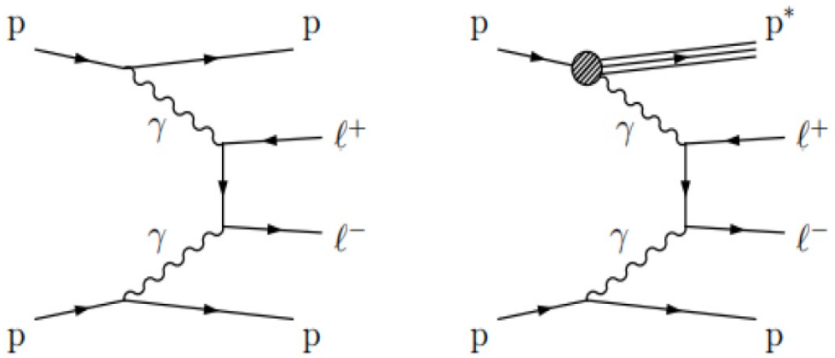

High-mass central (semi)exclusive production of lepton pairs at √s = 13 TeV

JHEP 07 (2018) 153

- First observation of proton-tagged $\gamma\gamma$ collisions at the EW scale
- 5.1$\boldsymbol{\sigma}$ significance reached with **2016 data** (9.4 fb^{-1})

JINST 18 (2023) P09009

Now an essential calibration handle:

- Select high-mass muon pairs produced back-to-back
- Use the correlation between di-muons and protons to validate the PPS proton reconstruction

PPS 2017+2018 data with 92.3 fb^{-1}

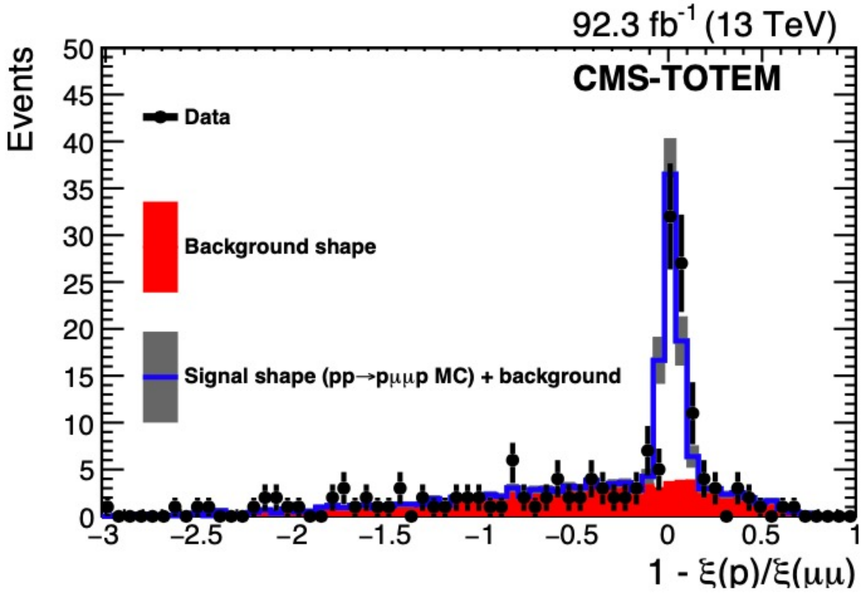

Correlation peak width consistent between data and simulation: **well described resolution**
Peak position at 0 as expected

Physics results – Run 2 data

$pp \rightarrow p \oplus \ell\ell \oplus p$

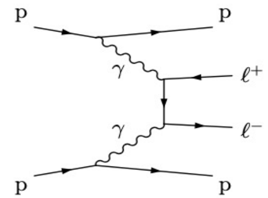

Observation of proton-tagged, central (semi)exclusive production of high-mass lepton pairs in pp collisions at 13 TeV with the CMS-TOTEM precision proton spectrometer
JHEP 07 (2018) 153 (doi)

$pp \rightarrow p \oplus \gamma\gamma \oplus p$

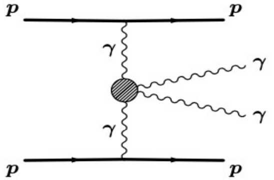

First search for exclusive diphoton production at high mass with tagged protons in proton-proton collisions at √s = 13 TeV
Phys. Rev. Lett. 129 (2022) 011801 (doi)

$pp \rightarrow p \oplus \gamma\gamma \oplus p$

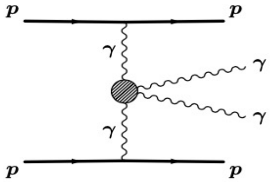

Search for high-mass exclusive diphoton production with tagged protons in proton-proton collisions at √s = 13 TeV
Phys. Rev. D 110 (2024) 012010 (doi)

$pp \rightarrow p \oplus VV \oplus p$

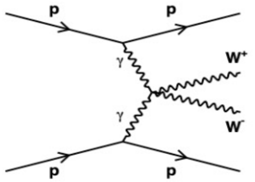

Search for high-mass exclusive γγ → WW and γγ → ZZ production in proton-proton collisions at √s = 13 TeV
JHEP 07 (2023) 229 (doi)

$pp \rightarrow p \oplus t\bar{t} \oplus p$

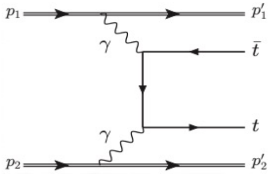

Search for central exclusive production of top quark pairs in proton-proton collisions at √s = 13 TeV with tagged protons
JHEP 06 (2024) 187 (doi)

$pp \rightarrow p \oplus ZX \oplus p$

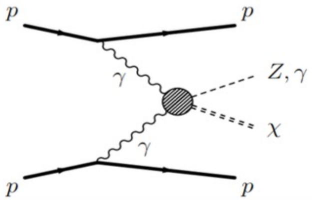

A search for new physics in central exclusive production using the missing mass technique with the CMS-TOTEM precision proton spectrometer
Eur. Phys. J. 83 (2023) 827 (doi)

Exclusive diphoton production - I

First analysis used 2016 data with 9.4 fb^{-1} (CMS 15.6 fb^{-1})
This analysis uses **full PPS Run 2 data with 103 fb^{-1}** (CMS 138 fb^{-1})

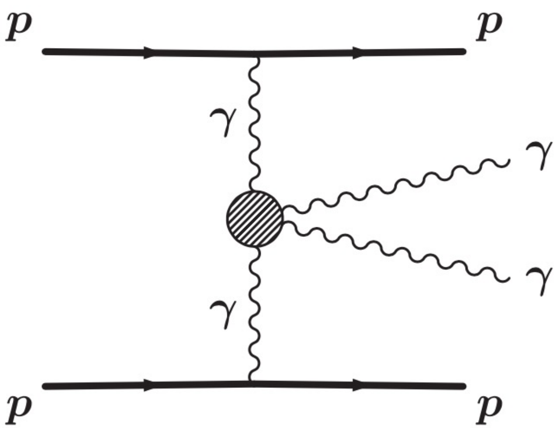

Search for **light-by-light (LbyL) events** in the diphoton **high-mass region**

Strategy, common for exclusive analyses:

- Select events with the CMS central detector, which are compatible with exclusive production
- Only consider events with protons measured in PPS
- Look for events with kinematics measured by the central detector matching that measured by PPS

Selection type	Criteria
Preselection	Diphoton HLT $p_T^\gamma > 75(100)$ GeV for 2016 (2017–2018) $H/E < 0.10$ Photon ID with electron veto $\lvert\eta^\gamma\rvert < 2.5$ (except $1.444 < \lvert\eta^\gamma\rvert < 1.566$, EB-EE transition veto) $m_{\gamma\gamma} > 350$ GeV
Acoplanarity	$A_\phi < 0.0025$
Diphoton $\xi_{\gamma\gamma}$	$0.02 < \xi^{\pm}_{\gamma\gamma} < 0.20$
Diproton ξ_p acceptance	$0.035 < \xi_p < 0.150$ (0.180) for sector-45 (sector-56)

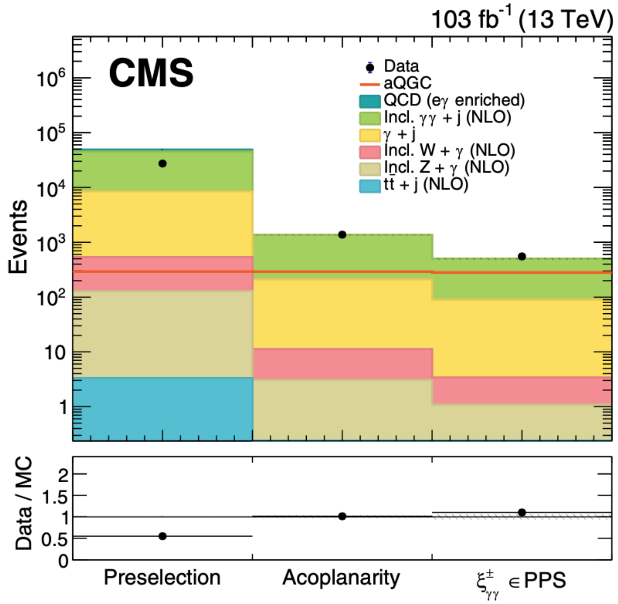

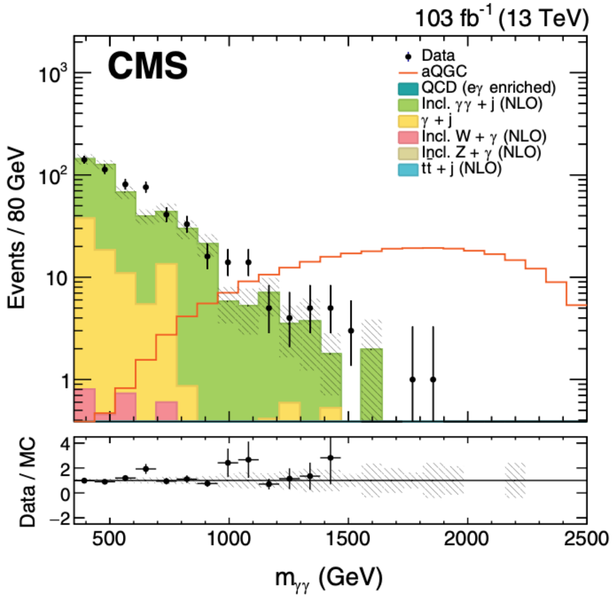

Exclusive diphoton production - II

Comparing the event kinematics measured from the diphoton system with that measured from the diproton one:

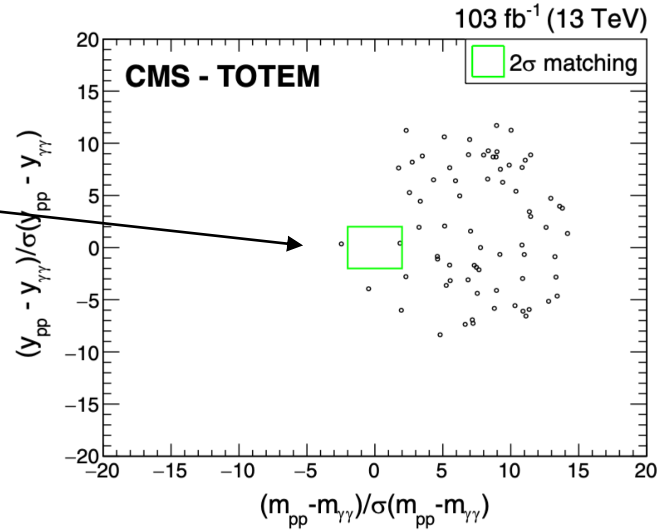

1 event observed with forward protons and 1.10 ± 0.24 events expected from background –> **No excess above SM prediction**

- Determination of **upper limit for cross section**:

$$\sigma\left(pp \to p\gamma\gamma p | \xi_p \in \xi^{\text{PPS}}\right) < 0.61\ \text{fb}$$

- **Set γγγγ AQGC limits in LbyL scattering** (best limits in this high-mass region):

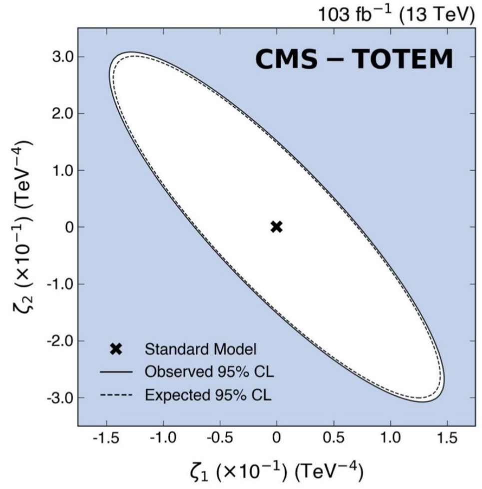

$$|\zeta_1| < 0.073(0.071)\ \text{TeV}^{-4}(\zeta_2 = 0),$$
$$|\zeta_2| < 0.15(0.15)\ \text{TeV}^{-4}(\zeta_1 = 0).$$

- **Set limit on axion-like particle production γγ -> a -> γγ** (best limit on ALPs coupling to γs in the 500-2000 GeV range):

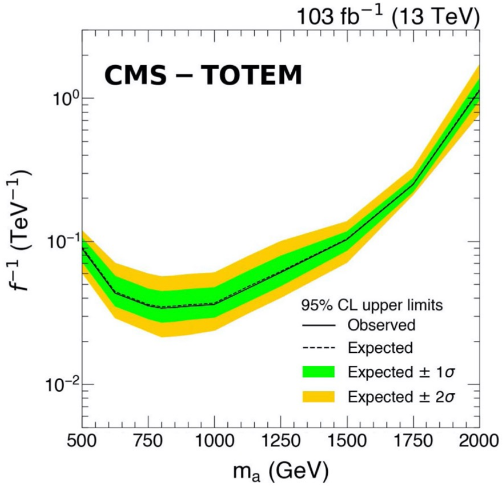

$$f^{-1} \approx 0.03 - 1\ \text{TeV}^{-1}$$
$$m_a \sim 0.5 - 2.0\ \text{TeV}$$

Exclusive WW and ZZ production - I

PPS Run 2 data with 100 fb^{-1} (CMS 138 fb^{-1}) in **fully hadronic decay channel**

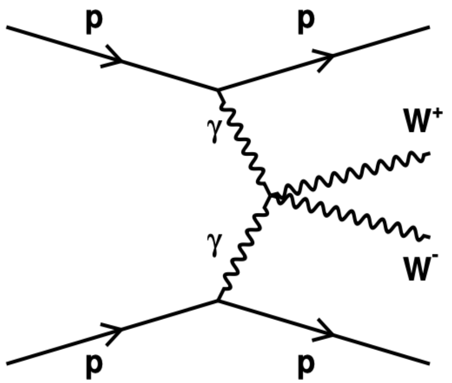

Search for **anomalous WW/ZZ (VV) exclusive production at high mass** exploring the hadronic decay channel (each V decaying into a boosted and merged jet)

SM production:

- ZZ not allowed at tree level
- WW exclusive production concentrated in the low mass region (High QCD background and out of reach with the Run 2 trigger thresholds on jets)

Event selection

- ≥2 V-tagged large-radius jets
- $p_T(j1)/p_T(j2)$ <1.3
- $|\eta(j1,j2)|$ <2.5
- $1-\Delta\phi(j1j2)/\pi$ <0.01
- $p_T(j1,j2)$ >200GeV
- 1126 GeV < $m(j1j2)$ < 2500 GeV
- $\eta(j1) - \eta(j2)$ < 1.3
- ≥ 1 proton per side of PPS

Signal regions:

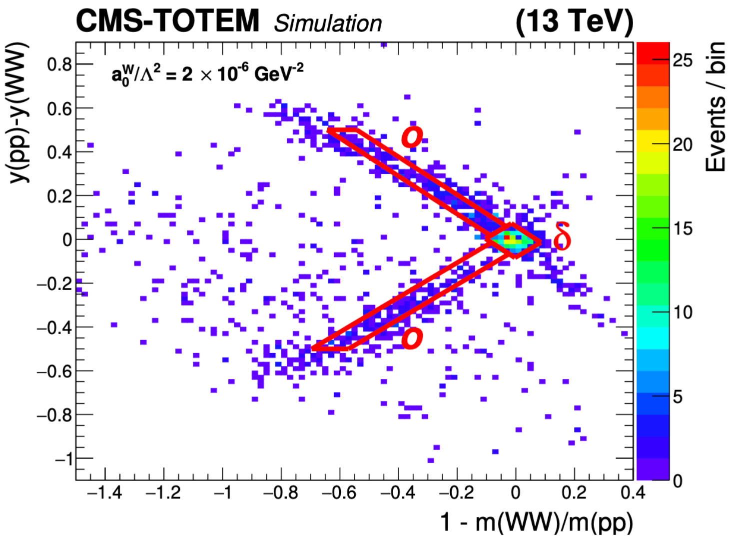

Mass match & Rapidity difference

ξ > 0.05 ; M_X < 1.55 – 2.10 TeV

$$m_{pp} = \sqrt{\xi^+\xi^- s} \qquad y_{pp} = \frac{1}{2}\log\left(\frac{\xi^+}{\xi^-}\right)$$

Two signal regions:

- δ : both protons from the interaction
- o : one proton mistakenly chosen from pileup

Exclusive WW and ZZ production - II

Observed data and expected number of background events
in each signal region for each data set (WW/ZZ & year)

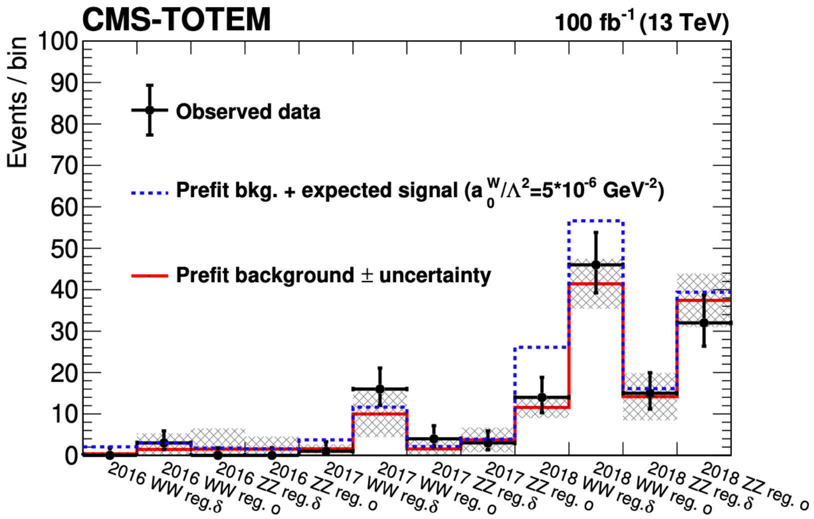

Hypothetical AQGC signals are also shown

Background: mainly QCD di-jet production combined with pileup protons

No significant excess observed

–> **fiducial cross sections for an AQGC-like signal in the pp → pWWp and pp → pZZp channels** :

$$\sigma(pp \to pWWp)_{0.04<\xi<0.20, m>1000\ \mathrm{GeV}} < 67(53^{+34}_{-19})\ \mathrm{fb}$$

$$\sigma(pp \to pZZp)_{0.04<\xi<0.20, m>1000\ \mathrm{GeV}} < 43(62^{+33}_{-20})\ \mathrm{fb}$$

Limits on γγVV AQGC in exclusive production:

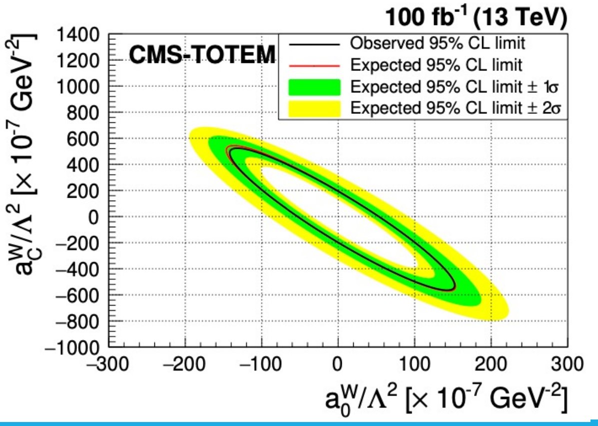

Coupling	Observed (expected) 95% CL upper limit No clipping	Observed (expected) 95% CL upper limit Clipping at 1.4 TeV
$\lvert a_0^W/\Lambda^2\rvert$	$4.3\ (3.9) \times 10^{-6}\ \mathrm{GeV}^{-2}$	$5.2\ (5.1) \times 10^{-6}\ \mathrm{GeV}^{-2}$
$\lvert a_C^W/\Lambda^2\rvert$	$1.6\ (1.4) \times 10^{-5}\ \mathrm{GeV}^{-2}$	$2.0\ (2.0) \times 10^{-5}\ \mathrm{GeV}^{-2}$
$\lvert a_0^Z/\Lambda^2\rvert$	$0.9\ (1.0) \times 10^{-5}\ \mathrm{GeV}^{-2}$	—
$\lvert a_C^Z/\Lambda^2\rvert$	$4.0\ (4.5) \times 10^{-5}\ \mathrm{GeV}^{-2}$	—

- Factor ~15-20 tighter limits on dim-6 $\gamma\gamma WW$ AQGC wrt Run 1 analysis without protons
- Limits converted to dim-8 operators, close to CMS same-sign $\boldsymbol{WW}$ and $\boldsymbol{WZ}$ results at 13 TeV after unitarization
- First limits on $\boldsymbol{\gamma\gamma ZZ}$ AQGC via exclusive $\boldsymbol{\gamma\gamma \to ZZ}$

Exclusive production of top quark pairs

PPS 2017 data with 29.4 fb^{-1}

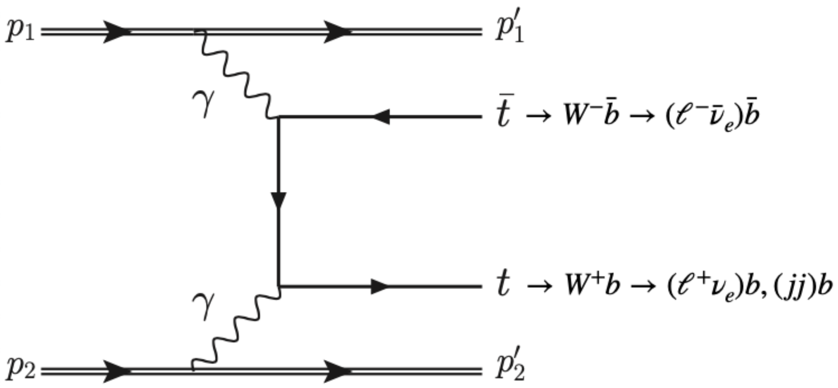

Low SM cross section (< 0.3 fb) in the PPS acceptance

–> no observation expected unless BSM physics enhances σ

–> derive upper limits

Two $t\bar{t}$ decay channels studied: *ℓℓ* and *ℓ*+jets

- $t\bar{t}$ selection: $p_T(j) > 30(25)$ GeV, $l+l$ (l+jets)

  $p_T^{leading}(l) > 30$ GeV ; $|\eta(l)| < 2.1$

  $M_{ll'} > 20$ GeV ; if $l=l'$: M_{ll} outside Z peak

  l + jets : 2 b-tag jets + 2 light-flavor jets

- **Proton matching**: $M_X = \sqrt{\xi^+ \xi^- s}$ $\quad y_X = \frac{1}{2} \log\left(\frac{\xi^+}{\xi^-}\right)$

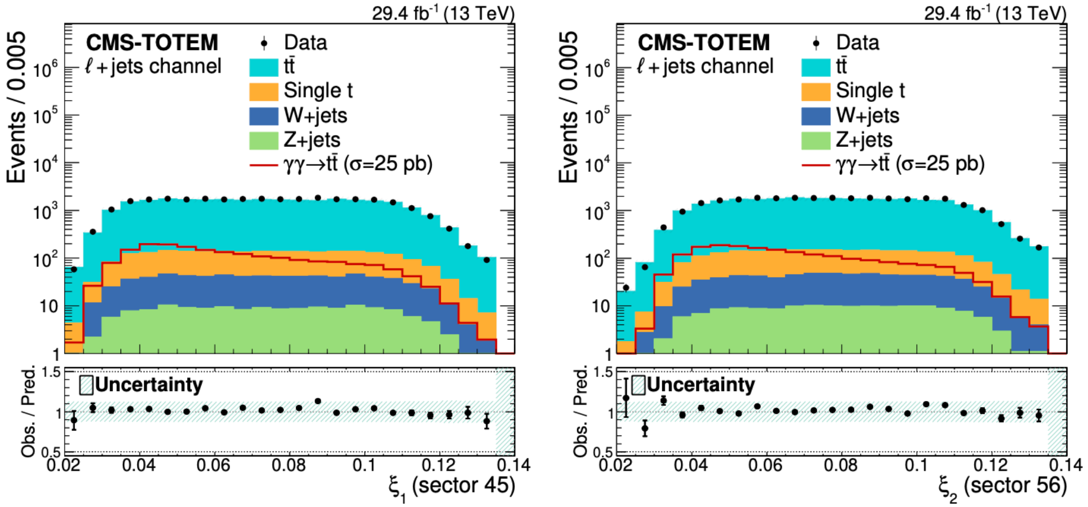

Cross section combined upper limit:

$\sigma_{t\bar{t}} < 0.59$ pb, 95 % CL

(expected 1.14 pb)

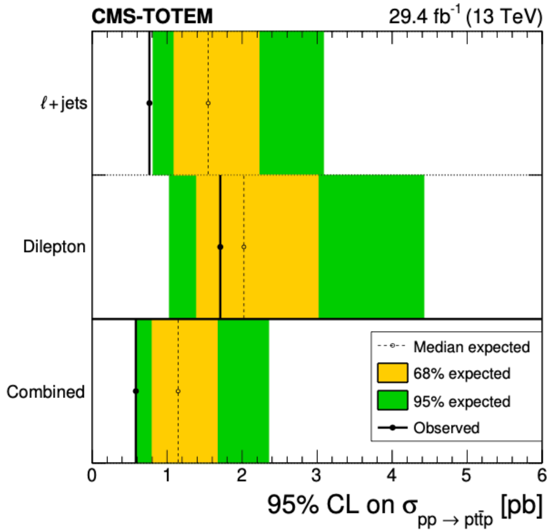

Exclusive ZX and γX production

PPS 2017 data with 37.2 fb^{-1}

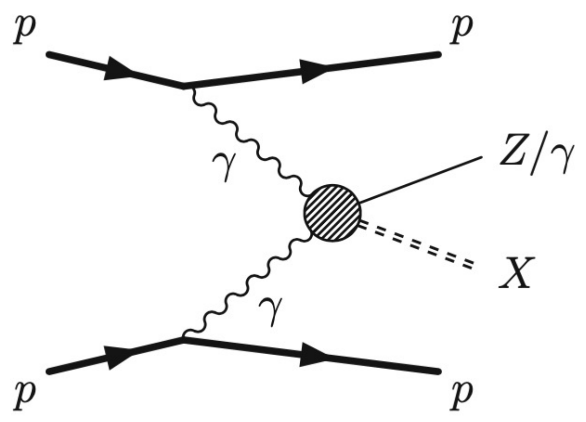

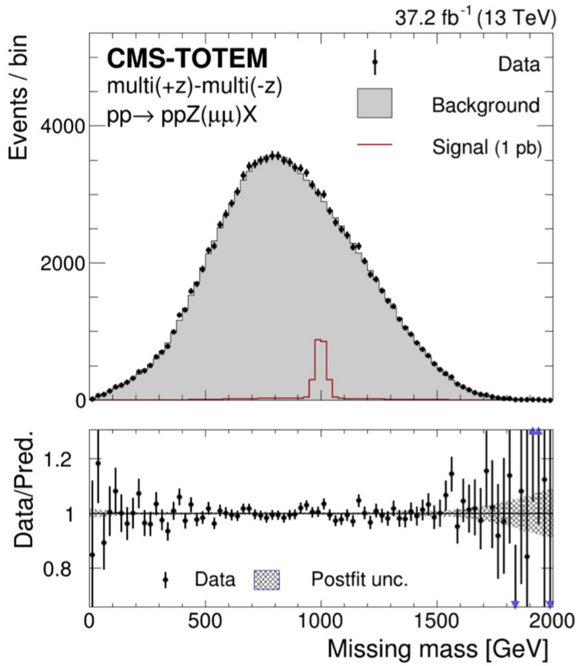

Novel "missing mass" technique to search for new particles, exploiting the high-precision proton momentum measurement from PPS:

$$m^2_{\text{miss}} = \left[(P^{\text{in}}_{\text{p}1} + P^{\text{in}}_{\text{p}2}) - (P_{\text{V}} + P^{\text{out}}_{\text{p}1} + P^{\text{out}}_{\text{p}2}) \right]^2$$

600 GeV < m_X < 1600 GeV – Excellent mass resolution of 2% (PPS+CMS)

- Dilepton decay channel $Z + X \rightarrow ll' + X$: ee : 948 070 events, $\mu\mu$: 1 477 237 events — > 99.7% from $Z \rightarrow ll$
- Photon channel $\gamma + X$: γ : 85 024 events — > 99.8% from single photon

Good background modelling based on data

Bump search over missing mass spectra gives no evidence of excess/deficit:

–> Data vs MC agreement better than 10%

95% CL upper limits on fiducial cross section

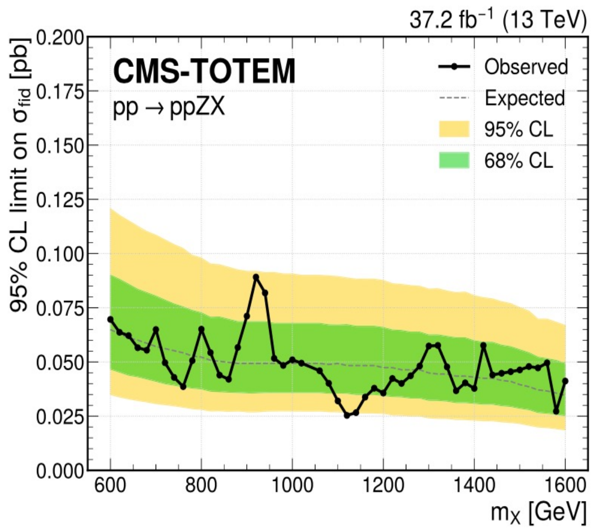

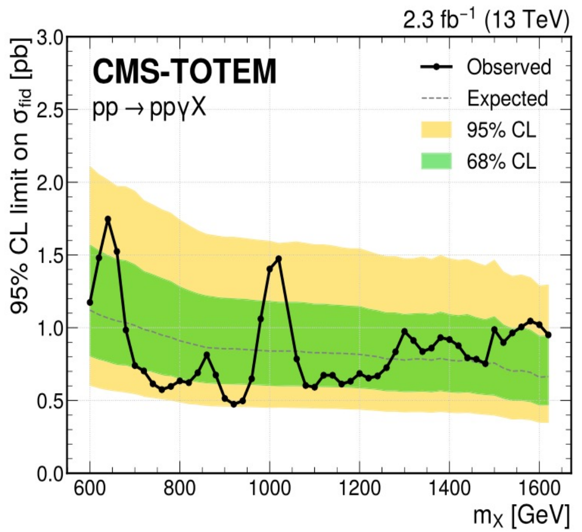

Physics with PPS Run 3 data

We plan to more than double our data after Run 3
Plenty of possibilities!

- **EWK**: LHC as $\gamma\gamma$ collider with tagged protons
  - Measurement of $\gamma\gamma \rightarrow W^+W^-$, e^+e^-, $\mu^+\mu^-$, $\tau^+\tau^-$
  - Search for aQGC with high sensitivity
  - Search for SM suppressed $ZZ\gamma\gamma$, $\gamma\gamma\gamma\gamma$ couplings
- **BSM**
  - Clean events (no underlying pp events)
  - Independent mass measurement by pp system
  - J^{PC} quantum numbers 0^{++}, 2^{++}
- **QCD**: LHC as gluon-gluon collider with tagged protons
  - Exclusive two- and three-jets events
  - Tests of pQCD mechanism of exclusive production
  - Gluon jet samples with small component of quark jet

Many analyses ongoing, stay tuned!

PPS2 at HL-LHC

HL-LHC aims at a peak luminosity of L_{peak} = 5 x 10^{34} $cm^{-2}s^{-1}$ to collect 3000 fb^{-1} of data

CMS is planning Phase-2 upgrades to be able to collect data at the rates imposed by the HL-LHC

PPS2 proposal for operation in the HL-LHC: CERN-CMS-NOTE-2020-008

✓ **Approved by CERN Research Board in September 2023 and included in the HL-LHC project**

Features:

- **Higher integrated luminosity**
  Most results will remain statistically limited even with Run 3 data
- **Larger central system mass acceptance range**
  - Current PPS double-arm acceptance: ~350 GeV – 2 TeV
  - HL-LHC will add acceptance up to 4 TeV
  - With vertical crossing angles (Run 4), reach lower masses ~200 GeV

PPS2 setup:

Choose best RP locations to exploit the new optics at HL-LHC:

–> **3 stations proposed** at 196, 220, 234 m **with tracking and timing detectors**

–> one less probable station at 420, not approved, very difficult because in cryogenic arc

See D. Druzhkin's talk on PPS2 tomorrow

PPS2 at HL-LHC – Acceptance

With detectors at the proposed positions of 196, 220, and 234 m, PPS2 is expected to have a **wide mass acceptance with the combination of different detector stations.**
Dependence on beam crossing angle α, levelling, β^*, apertures, …

Vertical Crossing-Angle				
Station	$\|\xi_{min}\|$	$\|\xi_{max}\|$	M_{min} [GeV] @ y = 0	M_{max} [GeV] @ y = 0
196 m	0.0786 – 0.0856	0.1967	1100.87 – 1197.80	2754.27
220 m	0.0371 – 0.0381	0.0688	519.89 – 533.18	962.70
234 m	0.0189 – 0.0095	0.0263	264.96 – 132.80	368.11
420 m	0.0031 – 0.0034	0.0116	43.38 – 47.04	162.66
Horizontal Crossing-Angle				
Station	$\|\xi_{min}\|$	$\|\xi_{max}\|$	M_{min} [GeV] @ y = 0	M_{max} [GeV] @ y = 0
196 m	0.1654 – 0.1779	0.2871	2316.15 – 2490.07	4018.94
220 m	0.0984 – 0.1014	0.1488	1377.48 – 1419.13	2083.04
234 m	0.0564 – 0.0312	0.0732	789.48 – 437.07	1024.60
420 m	0.0032 – 0.0034	0.0118	44.55 – 48.20	165.28

VERTICAL

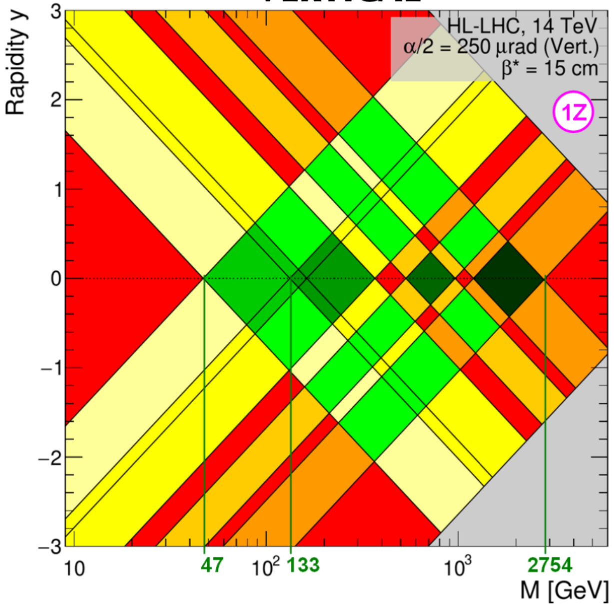

HORIZONTAL

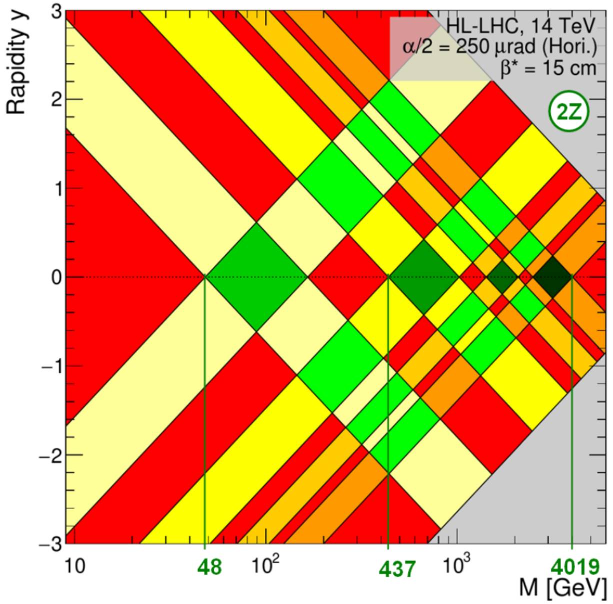

1Z / 2Z: extremes levelling trajectories

Vertical crossing angle preferred in terms of acceptance

PPS2 at HL-LHC – Physics perspective

PPS2 is an extraordinary opportunity at HL-LHC for CMS:

- No other equivalent detector (e.g. AFP) will be present
- Provides a unique extension to the CMS VBS/VBF physics program

Acceptance at low mass:

→ essential for SM measurements and spectrometer calibration

Highly dependent on the minimum ξ selection

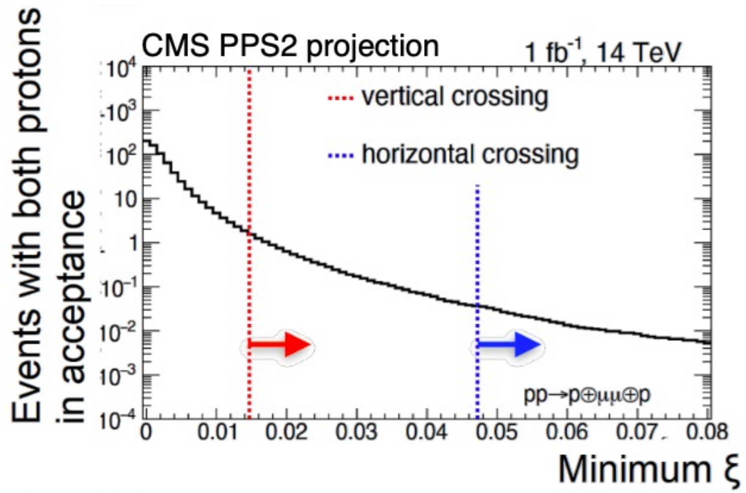

Many CEP channels to be studied:

- QCD physics: $pp \to p + jj + p$
- EWK physics: $pp \to p + WW/\ell^+\ell^- + p$
- Top physics: $pp \to p + tt + p$
- Higgs physics: $pp \to p + HWW + p$

Acceptance at high mass:

–> **key for BSM searches**

Indirect searches: $\gamma\gamma \to \gamma\gamma, \gamma\gamma \to WW, \gamma\gamma \to ZZ, \gamma\gamma \to \gamma Z$

Look for enhancements at high mass (AQGC)

Direct searches: Very good sensitivity to ALPs ($\gamma\gamma \to X \to \gamma\gamma$)

Search for invisible particles via the missing mass technique

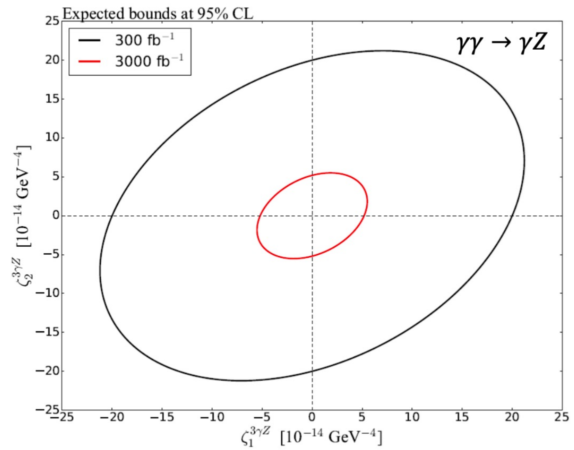

Summary

- **PPS has proven the feasibility of continuously operating a near-beam proton spectrometer at a high-luminosity hadron collider**

- **The PPS proton tagging capabilities are opening up new analysis strategies for CMS**
  –> rich program of physics analyses!

- **PPS is taking Run 3 data with the goal of more than doubling the integrated luminosity**

- **PPS2 will take part in HL-LHC**
  - ✓ A lot of physics potential to exploit
  - ✓ A unique opportunity at HL-LHC

Backup

PPS experimental apparatus (Run 2 – 2018)

- **PPS → High Luminosity Runs**
  - 2 pots with 3D Silicon Pixels for Tracking
  - 1 pot with 2 Diamond + 2 Double-Diamond planes for Timing
- **CMS-TOTEM → Low Luminosity special Runs**
  - 2 pots with Silicon Strip planes for Tracking
  - 1 pot with UFSD planes for Timing

6 planes of 3D Silicon Pixel Detectors **[H]**

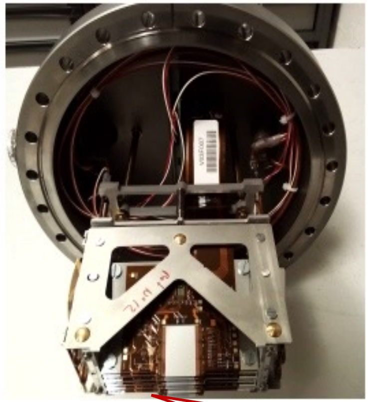

2 planes of Diamond + 2 planes of Double Diam. Detectors **[H]**

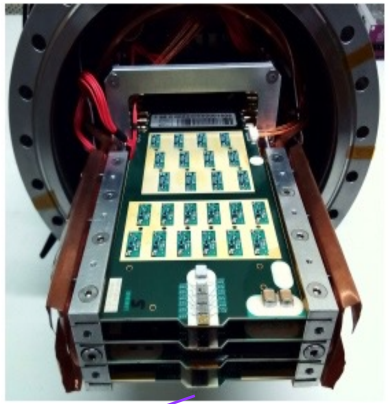

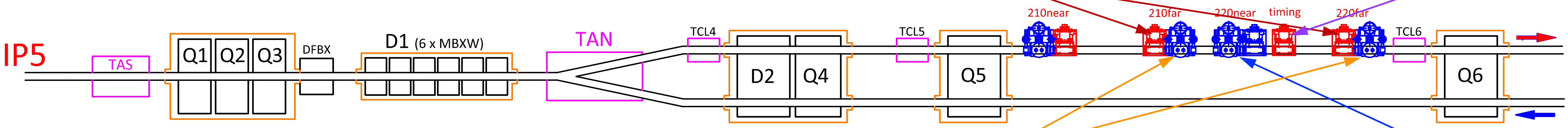

[H] PPS Horizontal Roman Pots
for high lumi - low β* runs
(high PU)

[V] CMS-TOTEM Vertical Roman Pots
for low lumi - high β* runs
(low PU)
→ to access central exclusive production of low mass systems

10 planes of Silicon Strip Detectors **[V]**

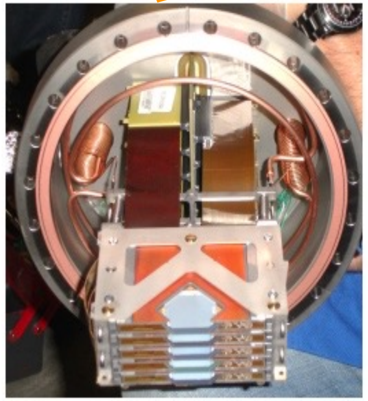

4 planes of UFSD **[V]**

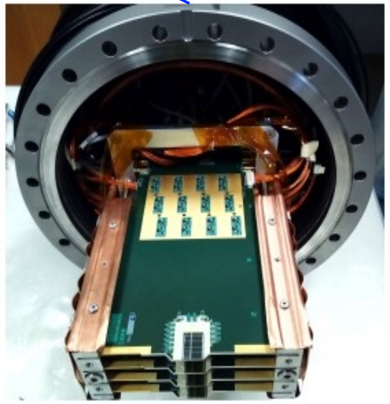

Detectors

Tracking detectors

- Aim: measure proton momentum
  - Detailed knowledge of the LHC optics required
- Technologies:
  - **Silicon Strips**
  - **3D Silicon Pixels** (radiation hard, high granularity and 'edgeless')

Strips

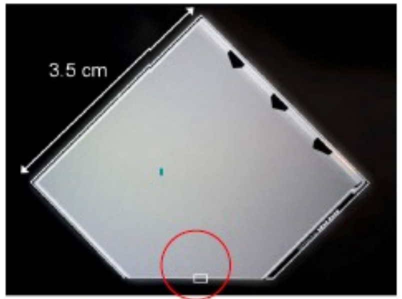

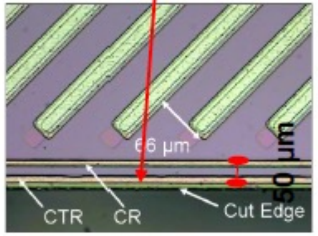

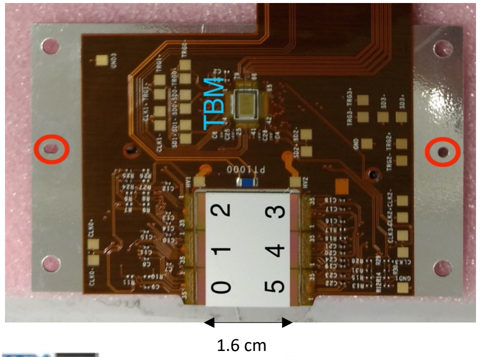

3D pixels

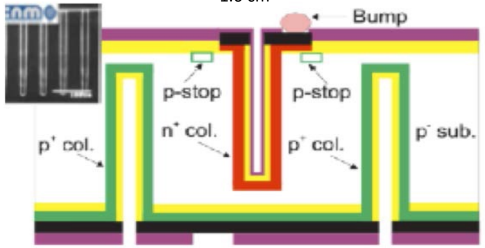

3D Run 2 (Double-sided)

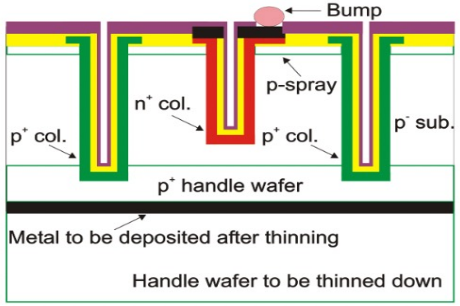

3D Run 3 (Single-sided)

Timing detectors

- Aim: disentangle primary vertex from pileup

$$\sigma_{z_{vtx}} = \frac{c}{2}\sqrt{2\sigma^2_{\Delta t}} \overset{\sigma_{\Delta t}=10\text{ps}}{\approx} 2\text{ mm}$$

$$\overset{\sigma_{\Delta t}=30\text{ps}}{\approx} 6\text{ mm}$$

$\sigma_{time} \sim 30$ ps $\rightarrow \sigma_Z \sim 6$ mm

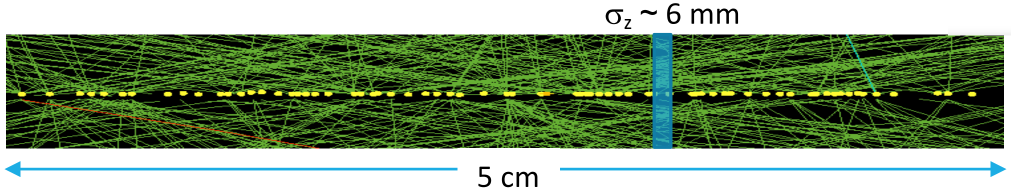

- Technologies:
  - **Single-diamonds (SD) and Double-diamonds (DD)**
  - **Ultra-Fast Silicon Detectors (UFSD) – 2017 only**

Diamonds

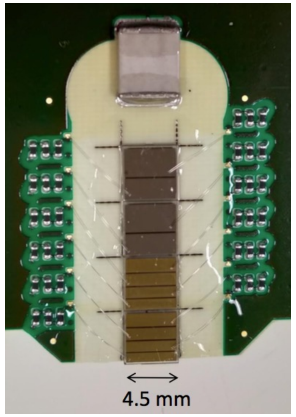

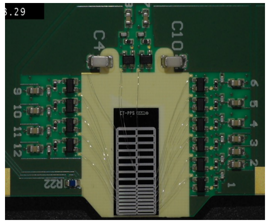

UFSD

Tracking detector - Silicon strips

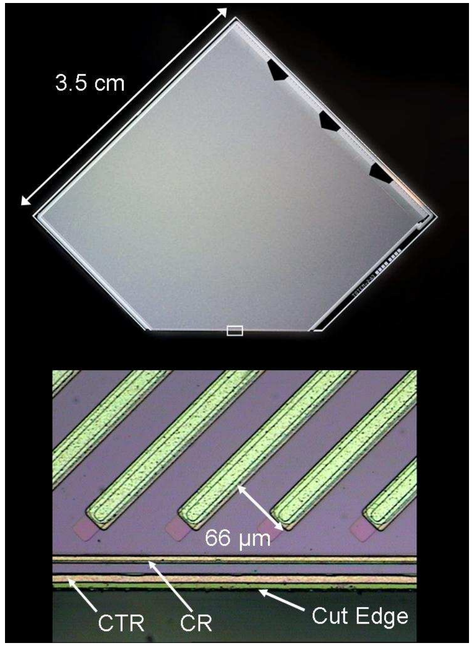

Same detectors used by the TOTEM experiment[*]

10 planes per pot of silicon strip detectors

- ▻ Micro-strip silicon detectors with edgeless technology (inactive edge ~50 µm)
- ▻ 512 strips at ±45°
- ▻ Pitch: 66 µm
- ▻ Digital readout provided by VFAT2 chips
- ▻ Lifetime up to an integrated flux of 5×10^{14} p/cm^2
  - ⟶ too low for PPS requirements, detector pushed to its limit
- ▻ Hit/track reconstruction using consolidated TOTEM algorithms (software fully integrated in CMS official software)
- ▻ No multitrack capability
- ▻ Track resolution ~12 µm

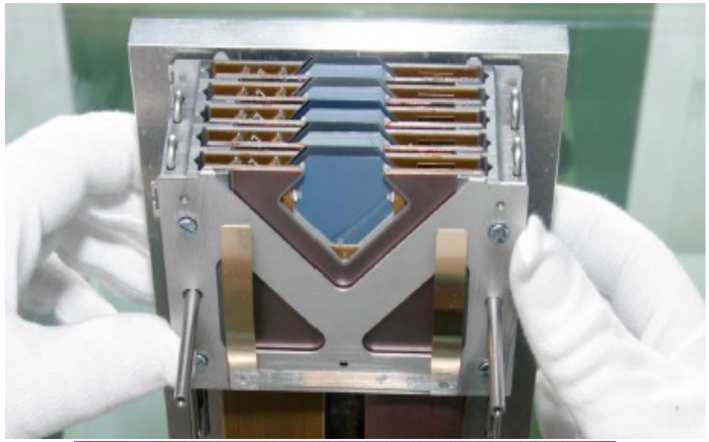

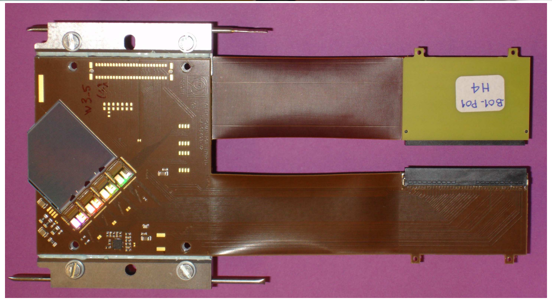

Planar technology + CTS
(Current Terminating Structure)

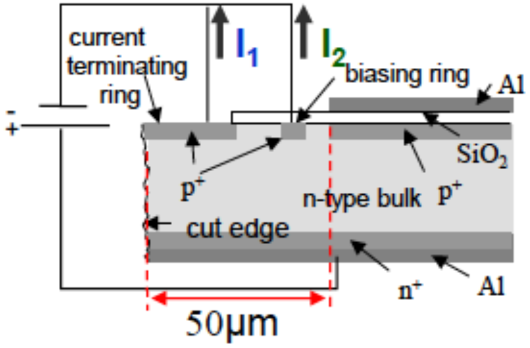

Simulation

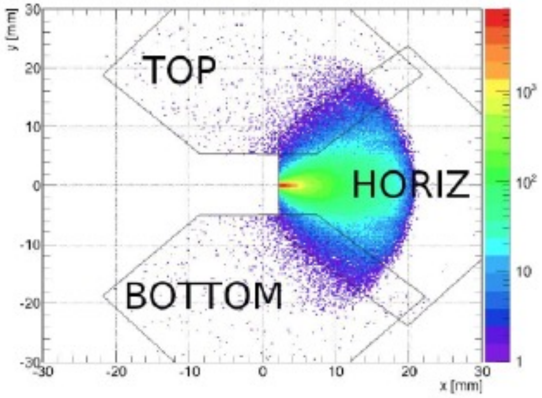

Data

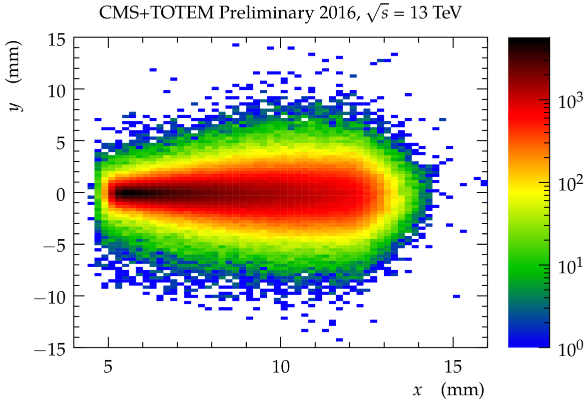

[*] TOTEM Coll., JINST 3 (2008) S08007

Si-strip detector efficiency (2017)

Two major sources of inefficiency (radiation damage and no multi-track capability) studied separately

[CERN-CMS-DP-2019-035]

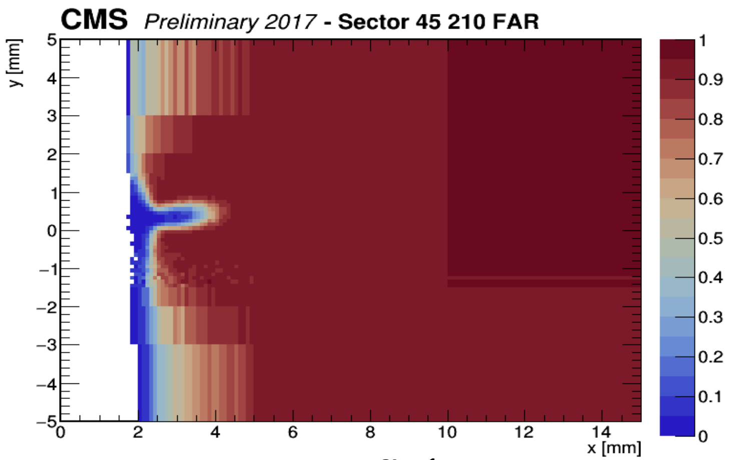

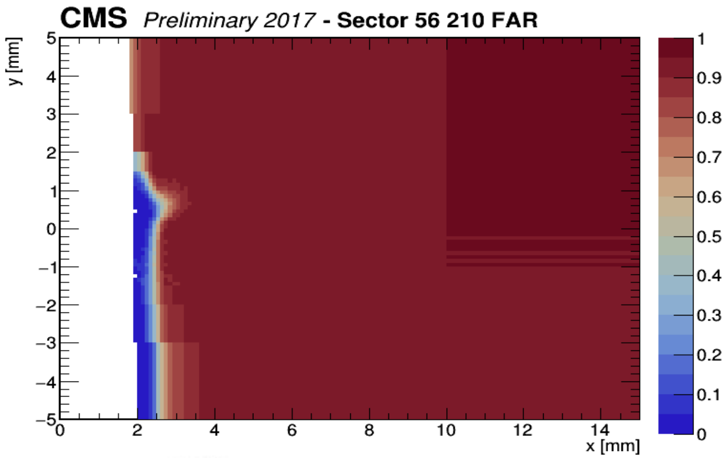

~ 9 fb^{-1}

Radiation damage in the area close to the beam is clearly visible

Efficiencies as a function of ξ are computed separately for each of the main LHC crossing angles used in 2017

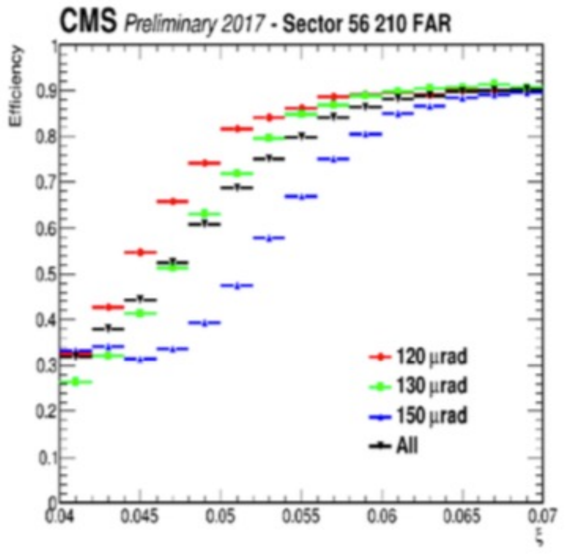

[CERN-CMS-DP-2018-056]

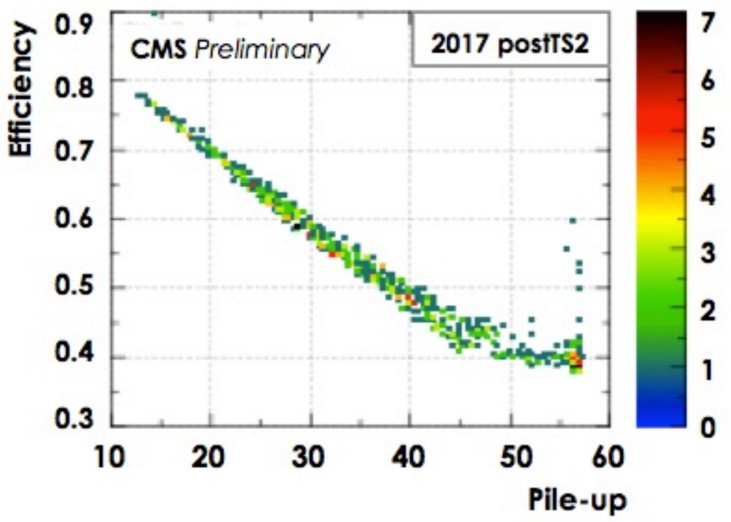

Only single-track events can be reconstructed with the strip detector

The increasing number of multi-track events with pileup shows the advantage of a pixel detector w.r.t. a strip one

Tracking detector - Silicon 3D pixels

6 planes per pot of 3D silicon pixel detectors

- ▻ 3D sensor in double-sided not fully passing-through technology
- ▻ Intrinsic radiation hardness → to withstand overall integrated flux of 5×10^{15} p/cm^2
- ▻ 200 µm slim edge → to approach the beam as much as possible
- ▻ Pixel dimensions: 100x150 µm^2 → very high granularity
- ▻ Resolution < 30 µm
- ▻ Planes tilted by 18.4° to optimize efficiency and resolution
- ▻ Front-end chip: latest version of PSI46dig[*], same as for the CMS Pixel detector
- ▻ Operation at about -20 °C and in vacuum (p < 20 mbar)
- ▻ Very good performance, bad pixels (efficiency < 90%) less than 0.05% of all channels

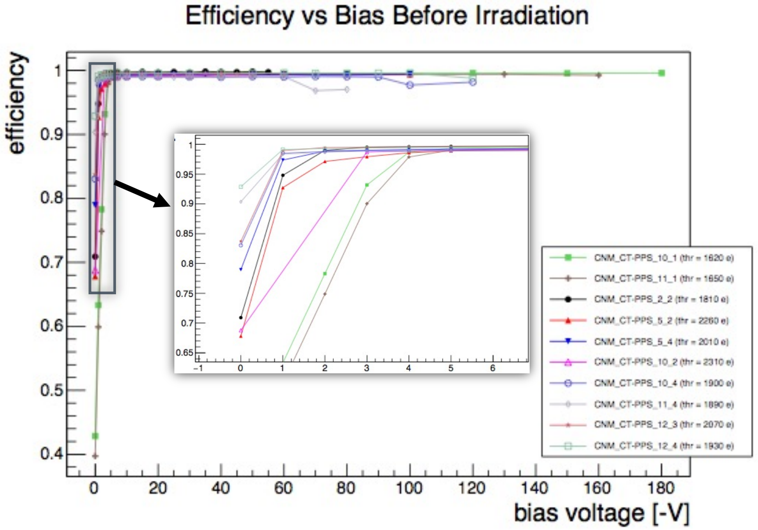

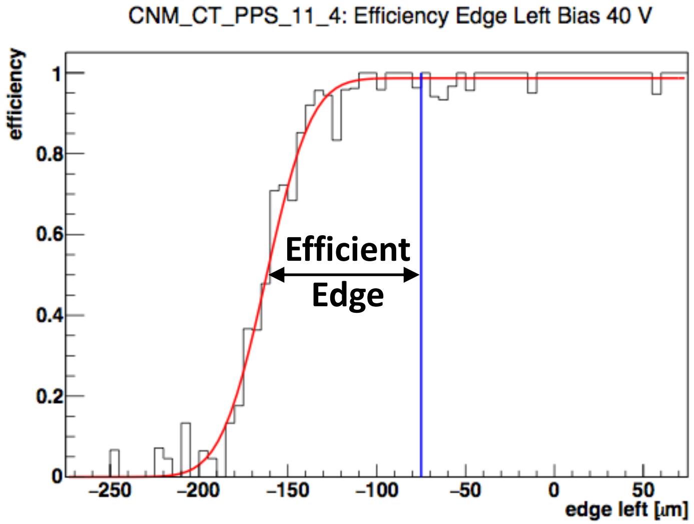

[*] F. Meier, PSI46dig pixel chip External Specification Manual (2013)

Silicon 3D pixel sensors in Run 2

3D sensor technology chosen because of its high radiation hardness and possibility to implement slim edges

Sensors produced by CNM with double-sided process and non-passing-through columns

Pixel size: 150x100

Sensor thickness: 230

Column depth: 200

Column diameter: 10

Depletion voltage: 5-10 V

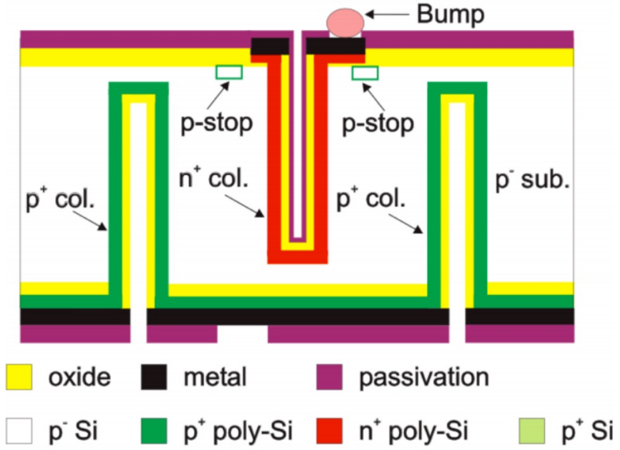

1E and 2E electrode layout

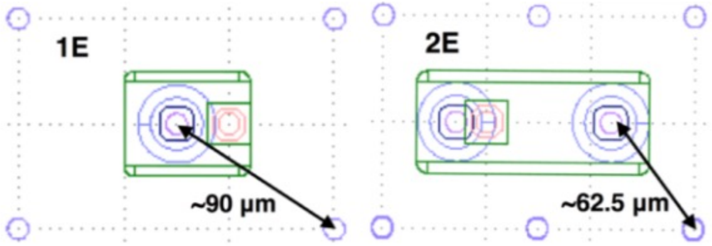

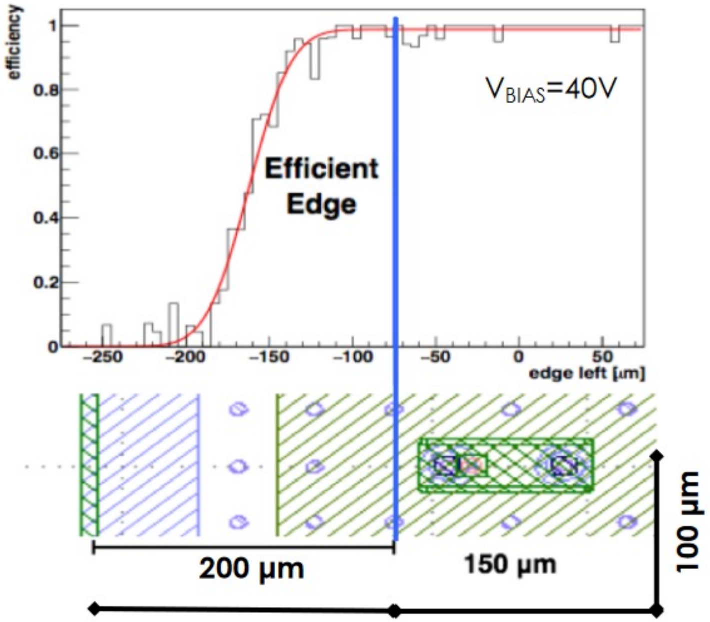

3D sensors bump-bonded to the PSI46dig ROC were extensively tested in laboratory and with beam, at FNAL [*]

- ✓ 200 slim edge made of triple p-type column fence. **Reduced to 50 by increasing the bias voltage** (for 2E type)
- ✓ **Spatial resolution for 2E**(1E) electrode configuration, with sensors tilted by 20°: **22** (25) µm

[*] F. Ravera, *The CT-PPS tracking system with 3D pixel detectors*, Pixel 2016 Workshop

Radiation damage of the 3D pixels readout chip

- ➢ The ROC used in CT-PPS is the same as that in layers 2-3-4 of the CMS central pixel detector
- ➢ The chip was not optimised for non-uniform irradiation
- ➢ After several irradiation tests, it has been understood that a non-uniform irradiation causes a difference between the analog current supplied to the most and the least irradiated pixels.
- ➢ The net result is that the amplified signal is slowed down and is associated to the following 25 ns clock window (BX):

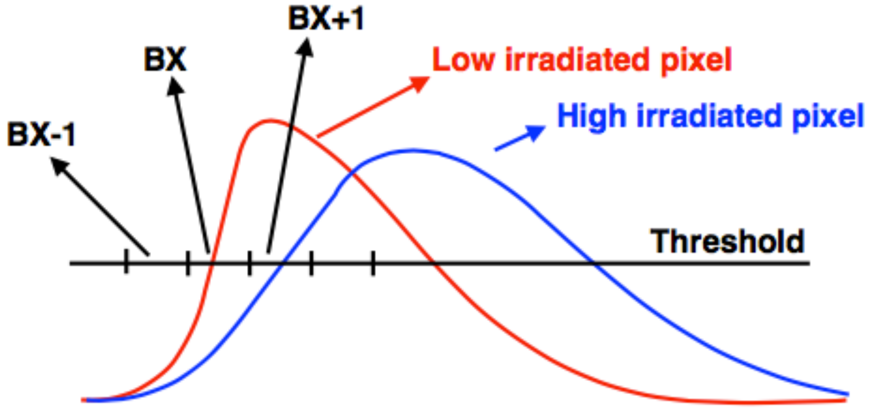

- ➢ The irradiation studies showed that the effect appears after an irradiation compatible with a collected integrated luminosity ~8 fb-1. To mitigate the impact on the data quality, the tracking stations have been lifted during Technical Stops to shift the occupancy maximum away from the damaged region

2D impact point distributions on tracking detectors

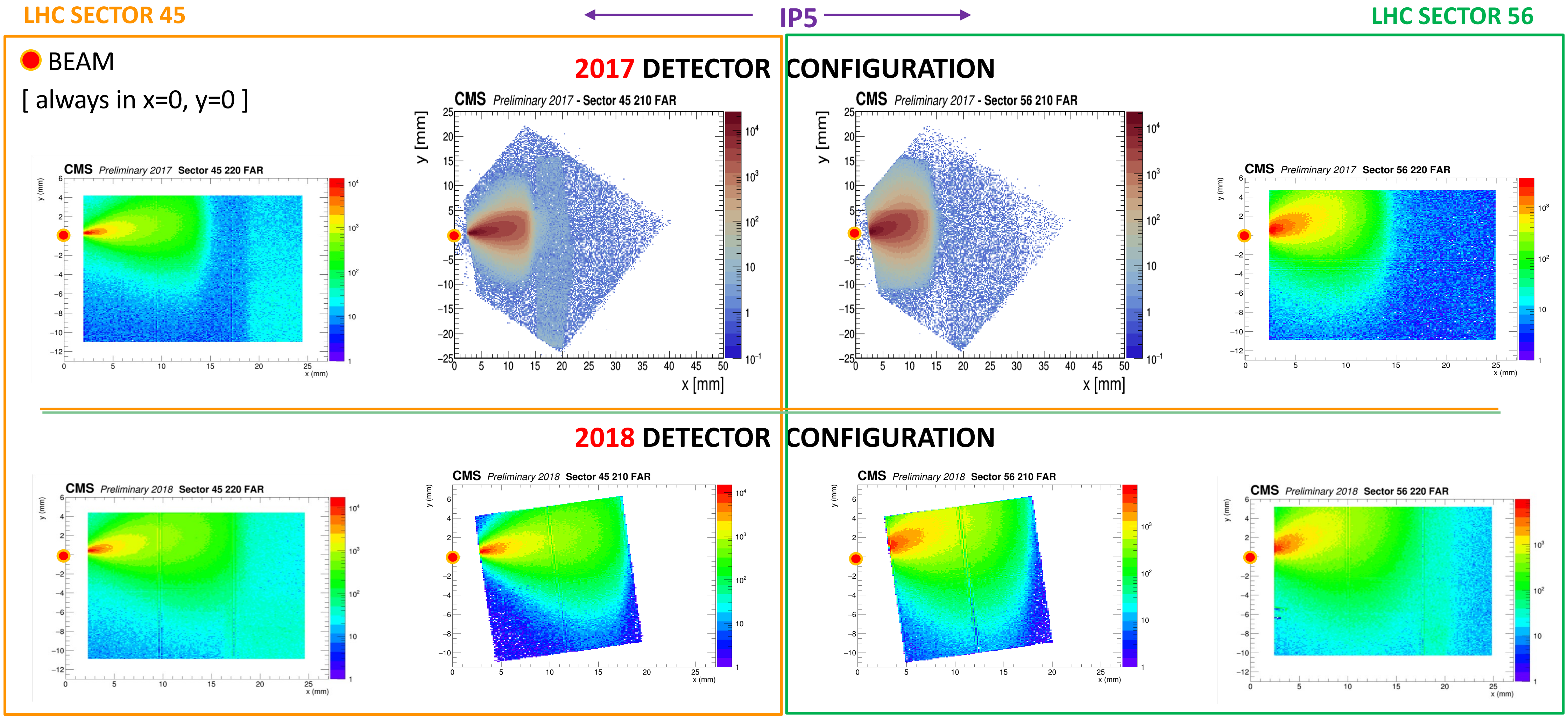

The RPs located at 210 m are tilted by 8° around the z axis.

3D pixel detector efficiency (2018)

Evolution of the RP efficiency maps in the detector region closest to the beam for RP 220 FAR (worst case)

BEGINNING OF DATA TAKING | TS | 21.0 fb^{-1} | TS | 50.3 fb^{-1} | 57.8 fb^{-1}

SECTOR 45

SECTOR 56

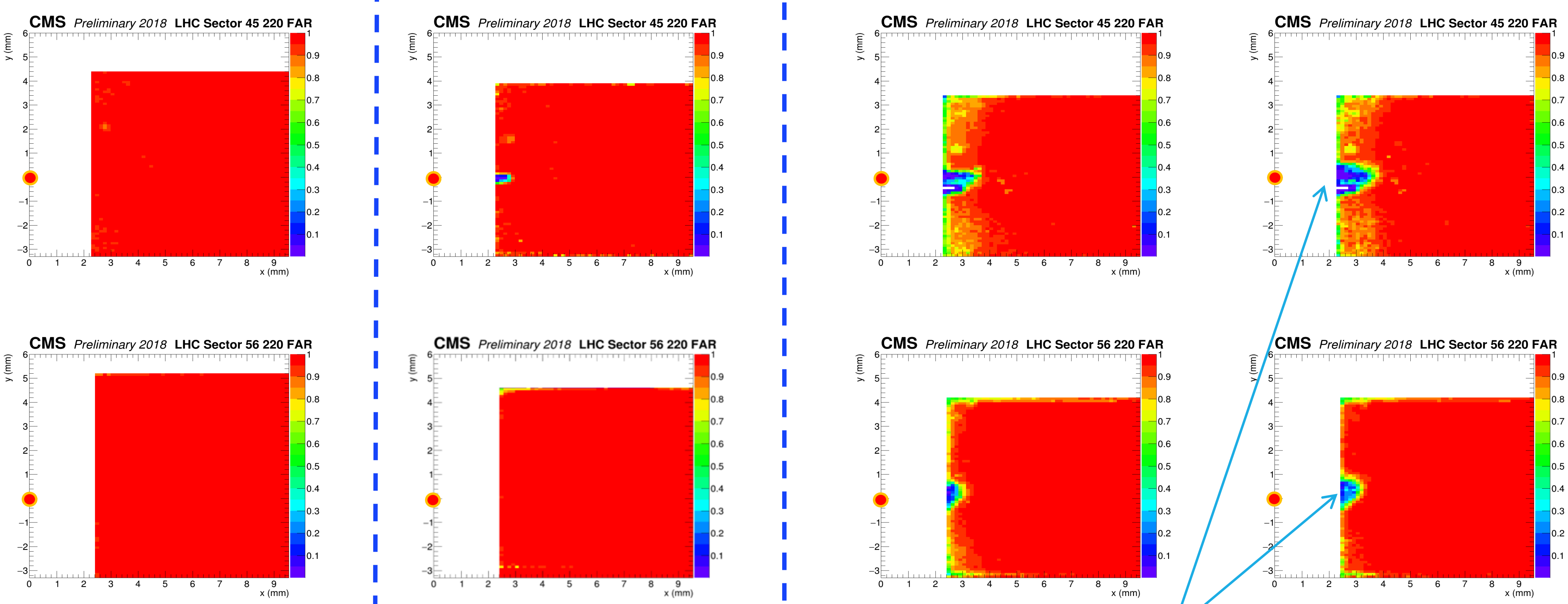

BEAM
[always in x=0, y=0]

RP SHIFTED BY 0.5 mm DOWNWARDS

RP SHIFTED BY 0.5 mm DOWNWARDS

Deterioration of the RP efficiency caused by the **radiation damage**

[CERN-CMS-DP-2019-036]

3D pixel detector efficiency (2018)

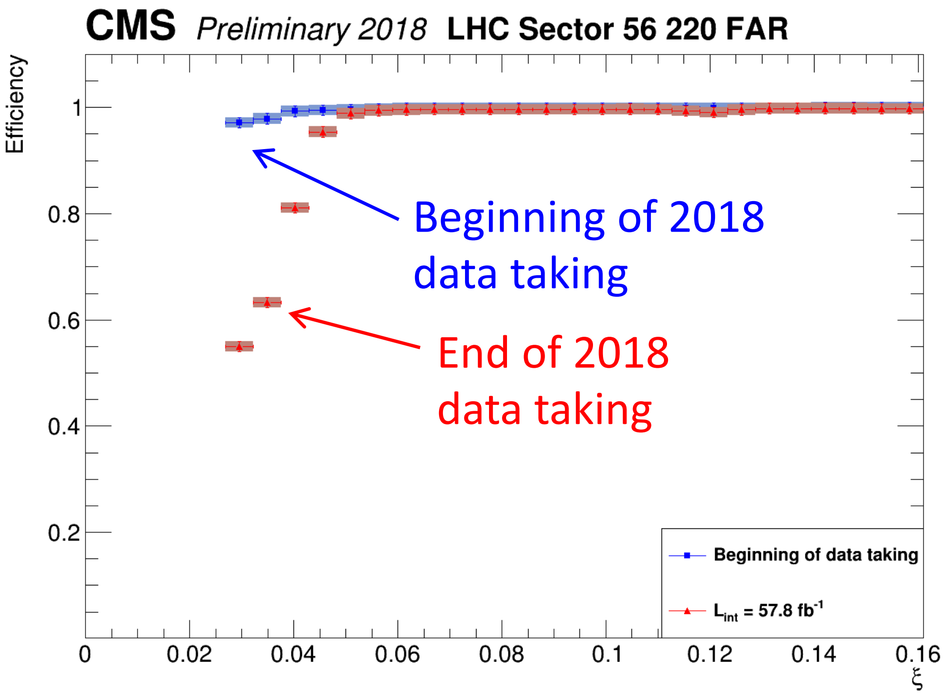

[CERN-CMS-DP-2019-036]

The **radiation damage** in the highest irradiated region **affects the detector performance at low ξ**

-> Impact on physics analyses, mainly at relative low masses of the central system X, not at high masses

Average efficiency calculated every 1 fb^{-1} in the critical region (irradiation peak area):

- **Recovery after each Technical Stop** (TS) because of the vertical movement of the RPs

Outside the irradiation peak area the efficiency remains high (>95%) and constant during all data taking

3D pixel tracker performance: hit resolution

Hit residuals for single planes are evaluated with respect to the local track reconstructed in the Pixel RP

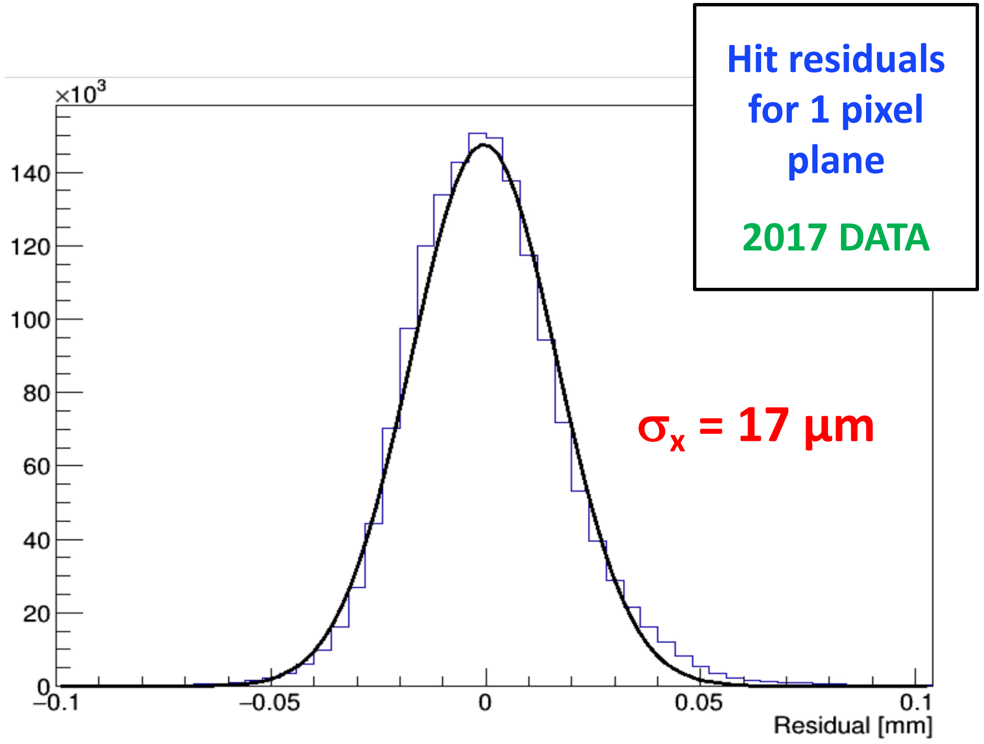

- Residuals are consistent with those obtained at the beam tests
- Similar results in 2018

✓ The pixel tracker works as expected

✓ Track resolution under final evaluation (~ 20 μm)

Tracking detectors in Run 3

PPS operates as a full CMS subsystem in LHC-Run3 (2022 - 2024)

TRACKER SYSTEM in LHC-Run3

- 2 Roman Pots per side, at 210 m and 220 m from CMS-IP, with 6 detector planes per RP
- New **3D silicon pixel sensors** produced by FBK
  - ✓ Single-side technology
  - ✓ 2x2 sensor geometry
  - ✓ 150 μm thick
  - ✓ 2E electrode configuration

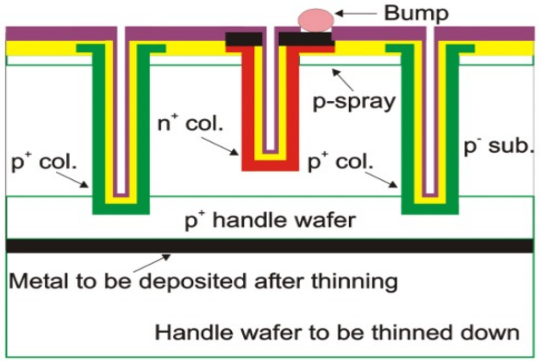

- ROC: **PROC600** (same as layer 1 of the CMS pixel detector)
- **New flex circuit design** (different 'look' but very similar design)
- **New detector package with internal movement system**, to better distribute the radiation damage

  → 12 positions spaced by 500 μm, possibility of handling more than 50 fb^{-1} with minimal efficiency loss

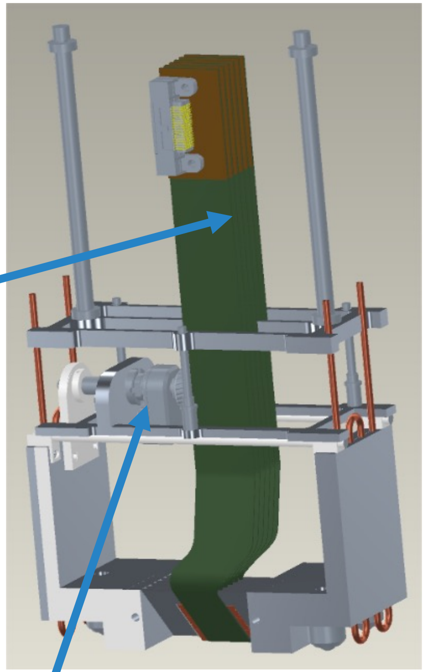

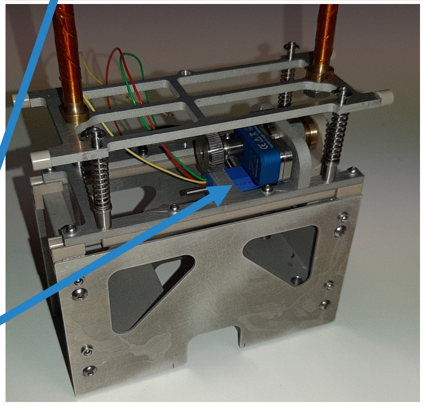

New flex circuit

Stepping motor

Movement system for the Run 3 tracker

Run 3 detector package heavily re-designed:

Sliding rails to allow ‘vertical’ movement

- ~6 mm range
- The package moves rigidly within the RP vessel

Stepping linear actuator + resistive position sensor

- Precise movement (resolution <10 μm)

Vertical movements to be performed during inter-fills

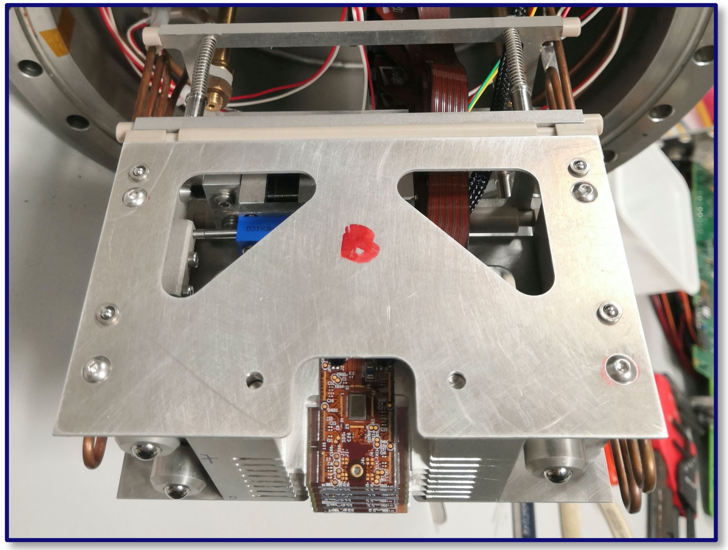

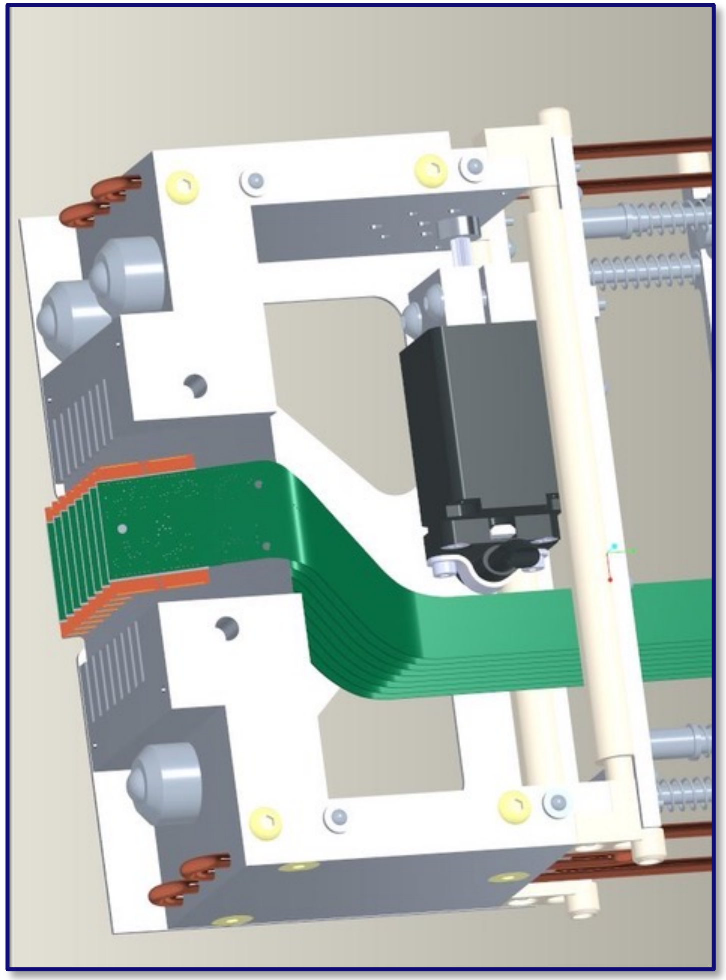

JINST 19 (2024) P05064

Timing detector - Diamonds

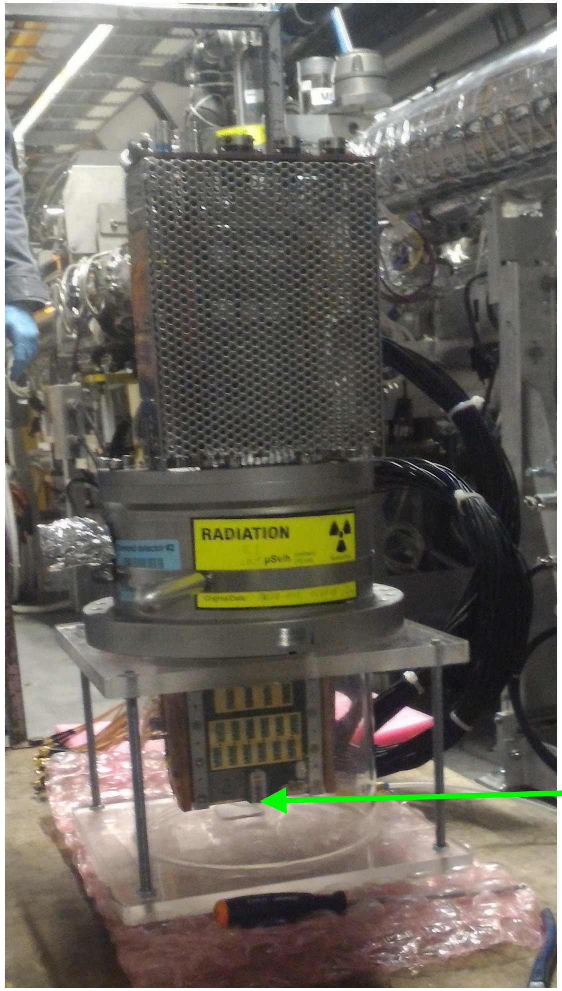

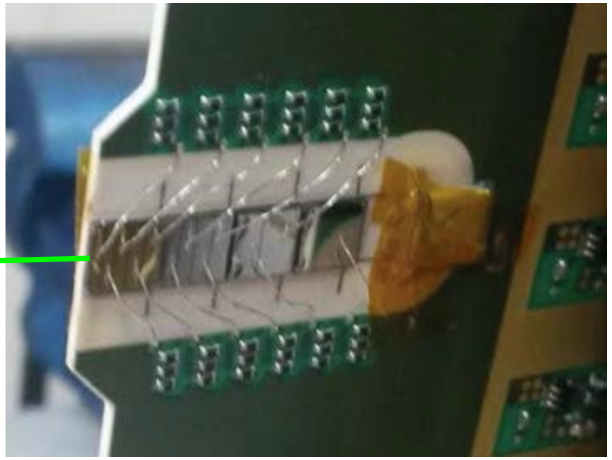

scCVD Diamond planes

- ▻ Four 4x4mm^2 diamond sensors per plane, 500μm thick, with different pad patterns
- ▻ Intrinsic radiation hardness → to withstand overall integrated flux of 5x10^{15} p/cm^2
- ▻ Allow for high granularity (wrt to, e.g., quartz)
- ▻ Time resolution ~ 80 ps per plane
- ▻ Amplification with TOTEM hybrid[1]
- ▻ Readout with NINO chip[2] + HPTDC[3]

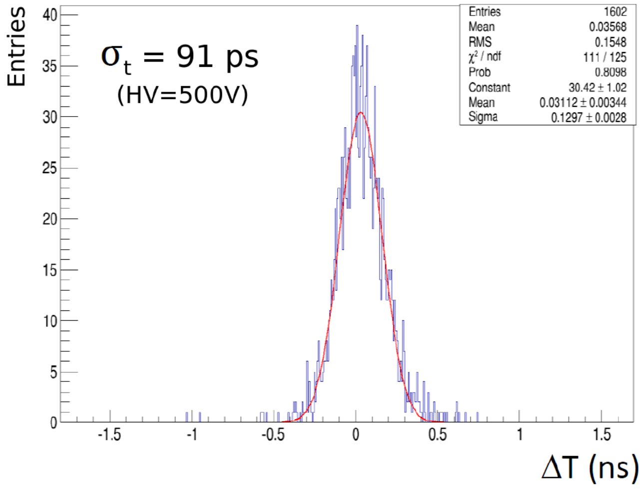

Time resolution for the detector prototype as measured in a test run in 2015

[1] TOTEM Coll., JINST 12 (2017) P03007
[2] F. Anghinolfi et al., NIM A 533 (204) 183
[3] M. Mota and J. Christiansen, IEEE JSSC 34 (1999) 1360

Timing detector - Double diamonds

Double-diamond planes
For improving the timing resolution of the diamond detector, two scCVD sensors (installed back to back) have been connected to the same amplifier channel, thus resulting in a timing resolution of 50 ps per plane as measured in a beam test[*].

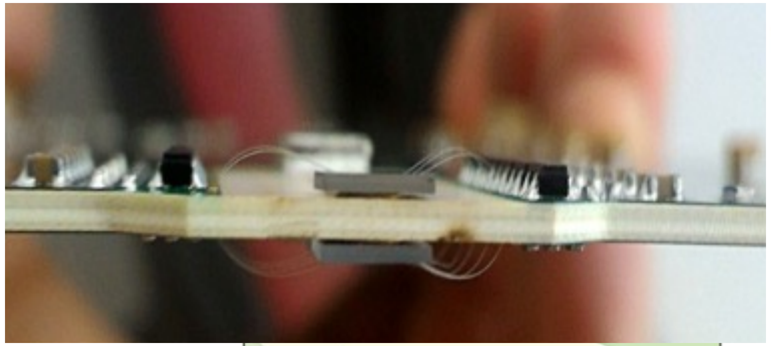

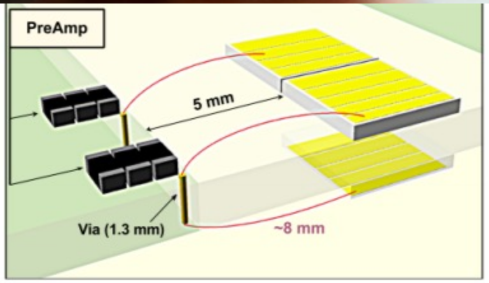

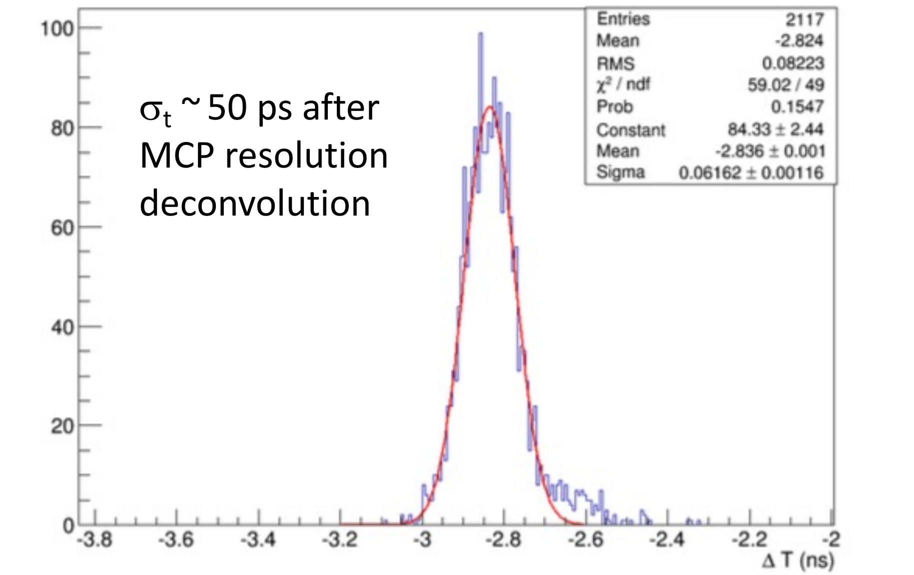

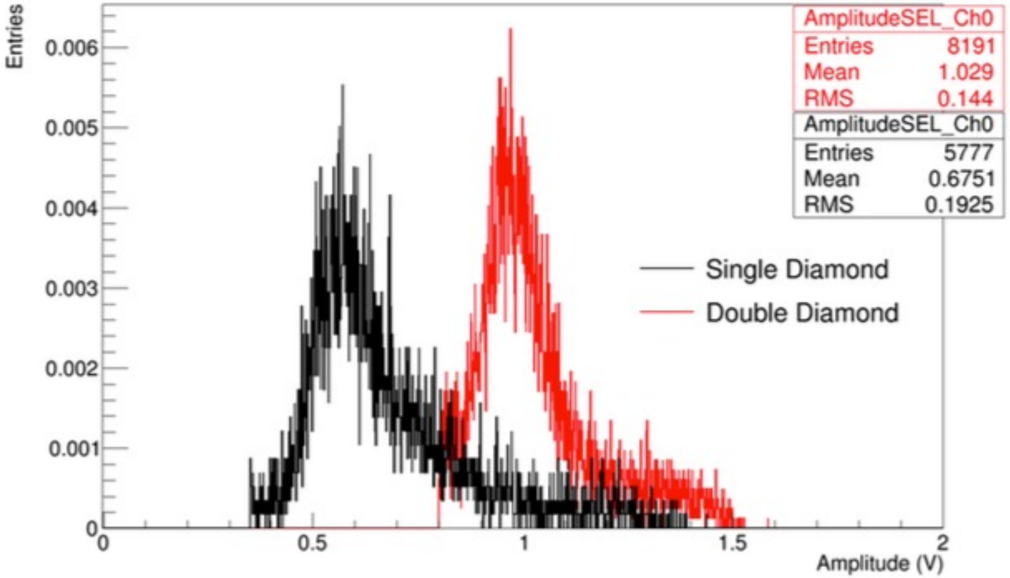

Signal from corresponding pads is connected to the same amplification channel:

- Higher signal amplitude
- Same noise (pre-amp dominated) and rise time (defined by shaper)
- Higher sensor capacitance
- Need a very precise alignment

Better time resolution w.r.t SD (factor ~ 1.7)

[*] M. Berretti et al., JINST 12 (2017) P03026

Time-track efficiency (Run 2 – 2018)

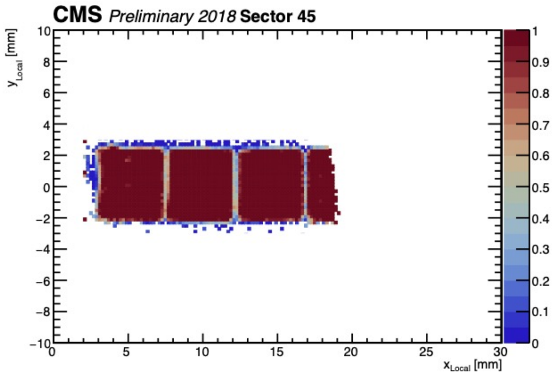

[CERN-CMS-DP-2020-046]

July 2018
Low PU

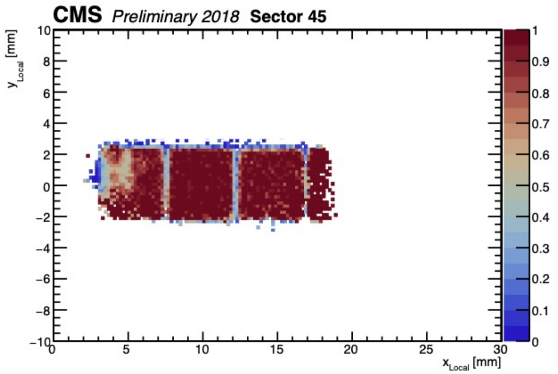

July 2018
High PU

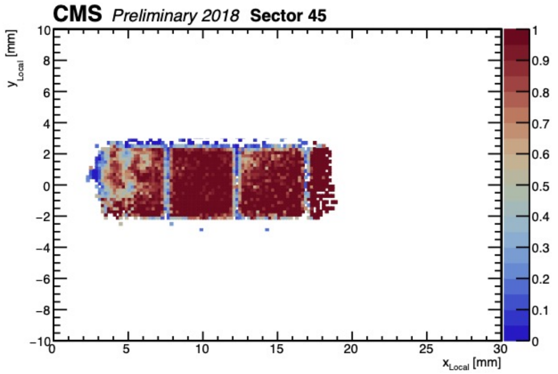

October 2018
High PU

Total efficiency of sensors + FE electronics + digitization + reconstruction

- Events with exactly 1 matched track in the pixel tracking stations are interpolated to find the expected track position in diamond timing detectors
- A search is performed for matching activity with a valid time-over-threshold measurement in the diamonds
- A minimum of 2 out of 4 planes on an arm is required to build a time-track

The time-track efficiency in low pileup data is near 100%

At the end of Run 2 (October 2018), the evolution shows a degradation of the efficiency, due both to localized reduced amplitudes from radiation damage, and to damage on the pre-amplifier electronics

Sensors have been re-tested in beam tests with optimized HV and LV conditions, with no degradation of the signal observed [CERN-CMS-NOTE-2020-007]

Proton timing resolution (2018)

This is a measurement of the **full timing station resolution** (sensors + front-end + digitization + timing channel calibration and reconstruction procedure)

[CERN-CMS-DP-2019-034]

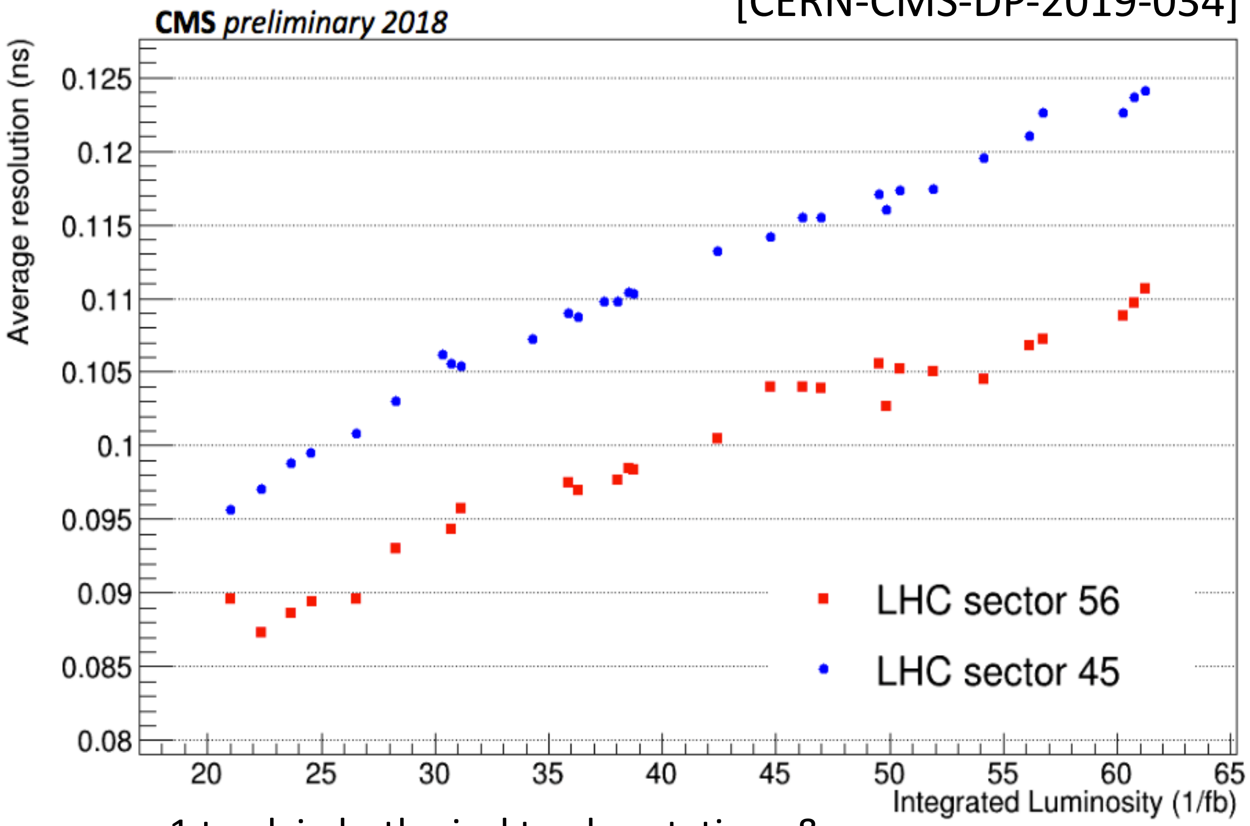

1 track in both pixel tracker stations &
4 diamond planes & 1 pad per plane

In 2018:
2 single-diamonds +
2 double-diamonds

Z_{PPS} vertex resolution (2018)

The resolution of the **full PPS timing system** (both arms) has been checked in central exclusive events collected in low pileup conditions during July 2018 [CERN-CMS-DP-2020-046]

$Z_{PP} = c\Delta t/2$

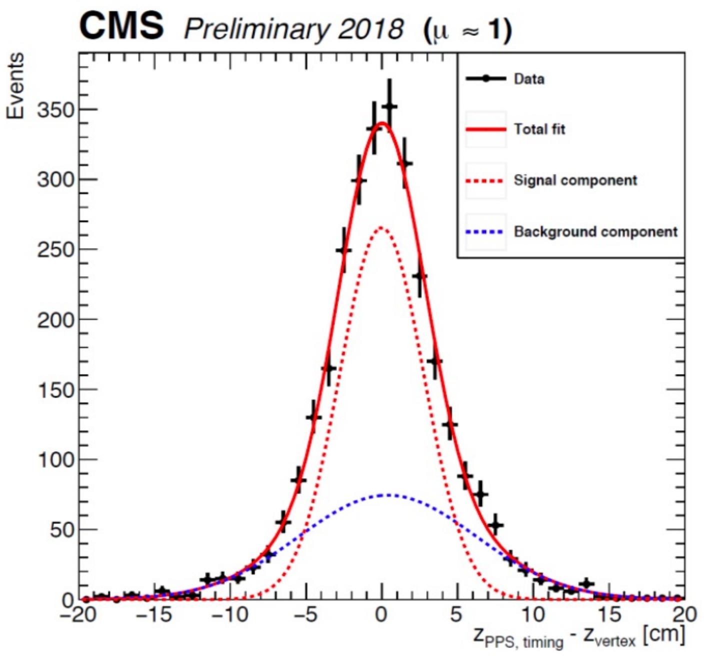

All timing tracks
σ_{Zpp} = (2.77 ± 0.17) cm

High resolution tracks
($\sigma_{track} < 100\ ps$):
σ_{Zpp} = (1.87 ± 0.21) cm

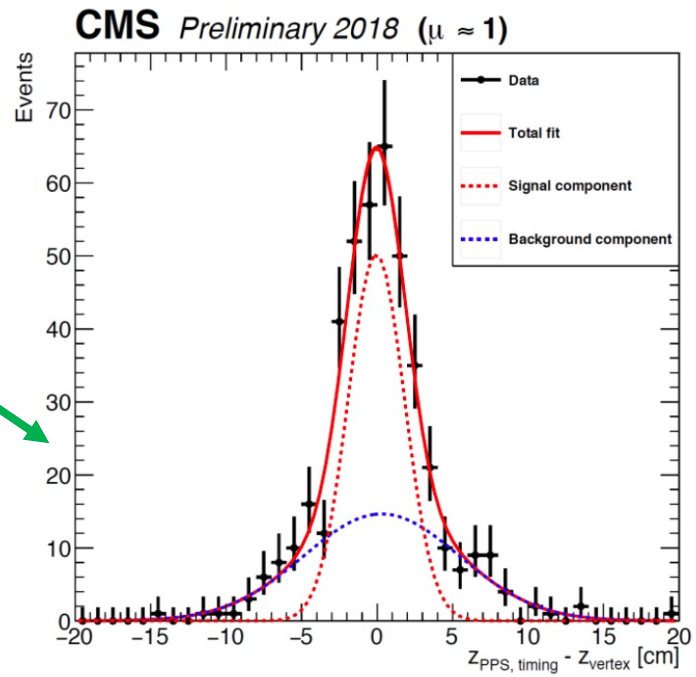

A strong correlation is observed between the time difference of the protons detected in PPS, and the longitudinal vertex position reconstructed in the central CMS tracker

Timing information can be used in physics analyses to suppress pileup background

Timing detectors in Run 3

An important upgrade program went on for the TIMING SYSTEM in LHC-Run3:

- **An additional timing station per sector** was built
  Each station is equipped with 4 DD planes → **8 DD planes in each sector**

- **New hybrid boards** -> increase in amplification stability and HV isolation, further optimization of performance
- **New discriminator board** (still based on NINO chip) -> reduce timing degradation in digitization phase
- Amplification LVs will be remotely controlled
- **Sensor readout with SAMPIC chip** (fast sampler @ 7.8 Gsa/s) available **for commissioning phase and sensor monitoring** (cannot sustain hit rate at nominal luminosity). Successfully used as CMS-TOTEM timing sensor readout for a special run in 2018 (lower hit rate, Ultra Fast Silicon Detectors as sensor) [PoS TWEPP2018 (2019) 137] :
  - ▻ Improvement of calibration quality
  - ▻ Fast feedback from settings modification
  - ▻ Monitor of sensor performance (disentangled from digitization stages)
  - ▻ Parallel readout -> No impact on regular data acquisition

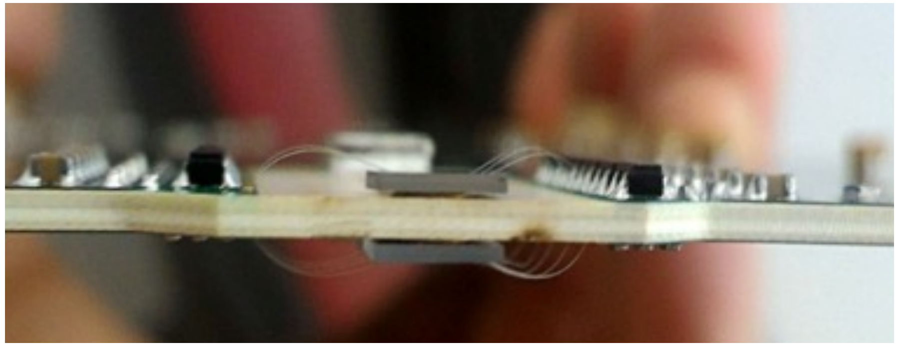

Ultimate resolution goal (< 30 ps) within reach

Timing detector - UFSD

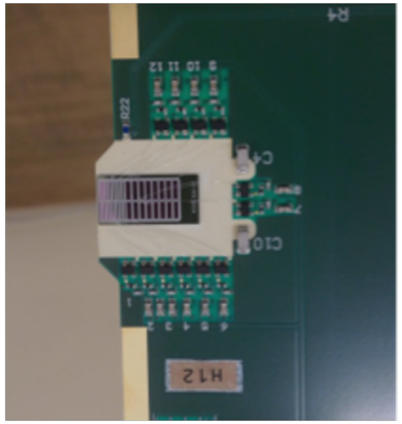

UFSD planes - **First installation in HEP, 1 plane in 2017**

- Eight 0.5x6mm^2 pads, four 1x3mm^2 pads
- Radiation hardness still an issue → in RP environment (T > 30°C) lifetime $\lesssim 10^{15}$ p/cm^2
- Allow for high granularity (wrt to, e.g., quartz)
- Time resolution ~ 35 ps per plane[*]
- Amplification with modified TOTEM hybrid[2]
- Readout with NINO chip[3] + HPTDC[4]

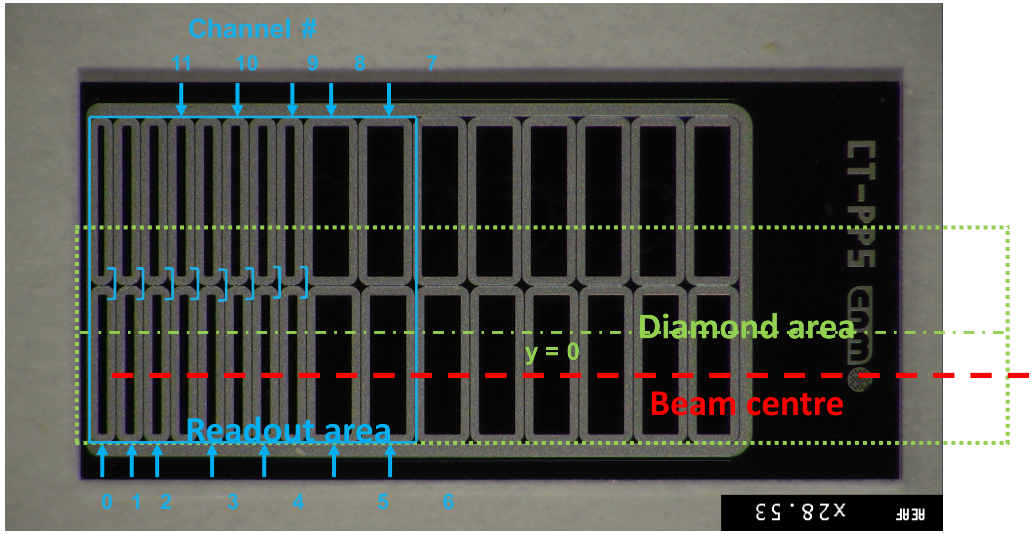

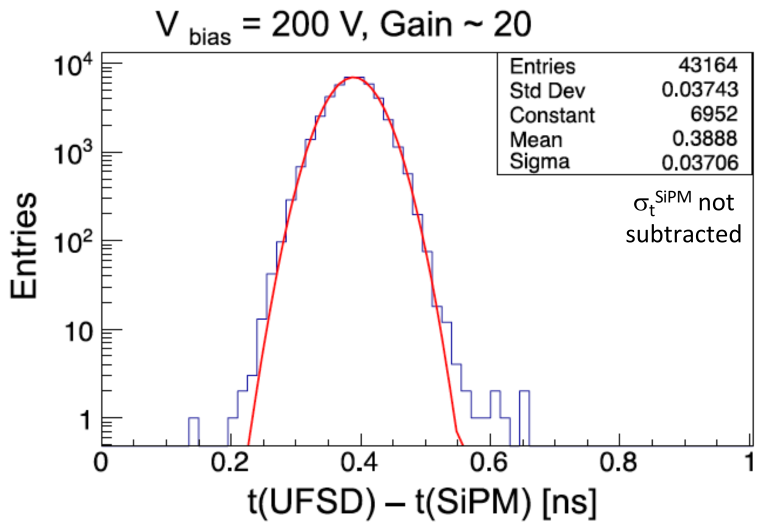

[*] N. Cartiglia et al., NIM A 850 (2017) 83

Proton reconstruction

The **proton reconstruction relies on**:

- the **alignment** of the detectors planes w.r.t. the LHC beam [CERN-TOTEM-NOTE-2017-001]
- the knowledge of the transport matrices parametrising the LHC magnet lattice, referred to as **beam optics** [CERN-TOTEM-NOTE-2017-002]

Starting from the **reconstructed hits** in the tracking detectors

↓ ← **Local alignment, done once among detectors in each pot**

local proton **tracks** are reconstructed

↓ ← **Global alignment with beam, done for each physics fill**
Optics knowledge

and the **proton kinematics** at the IP is derived

Alignment: special runs and physics fills

To validate each optics configuration, a **low intensity** "**alignment run**" is required where also the **TOTEM vertical RPs** approach the beam, allowing to align:

a) **the RPs (V and H) among themselves**

b) **the RPs with respect to the beam**, using a **sample of elastic protons** which are distributed symmetrically about the beam and detected in the vertical pots

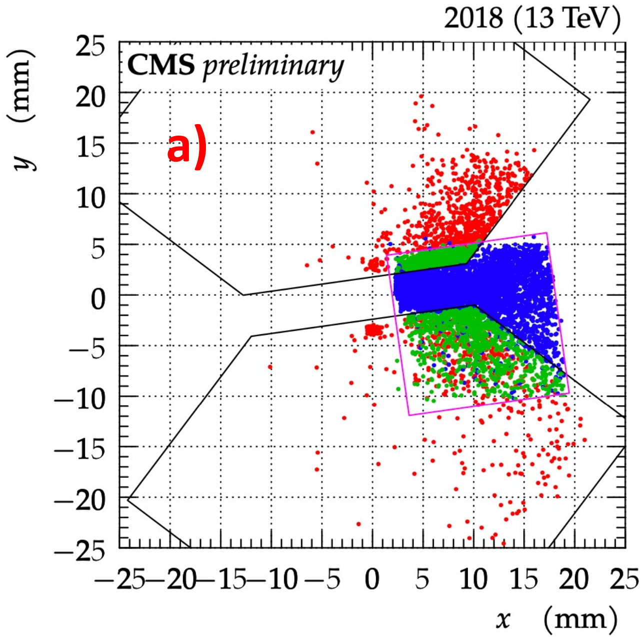

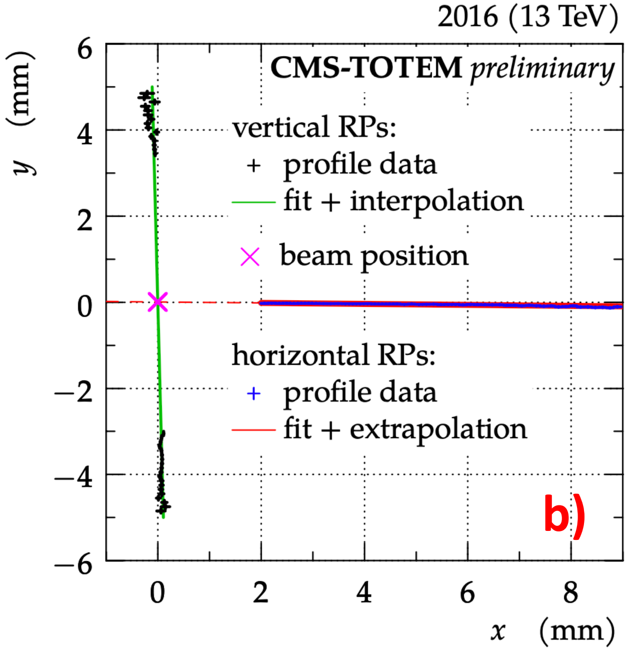

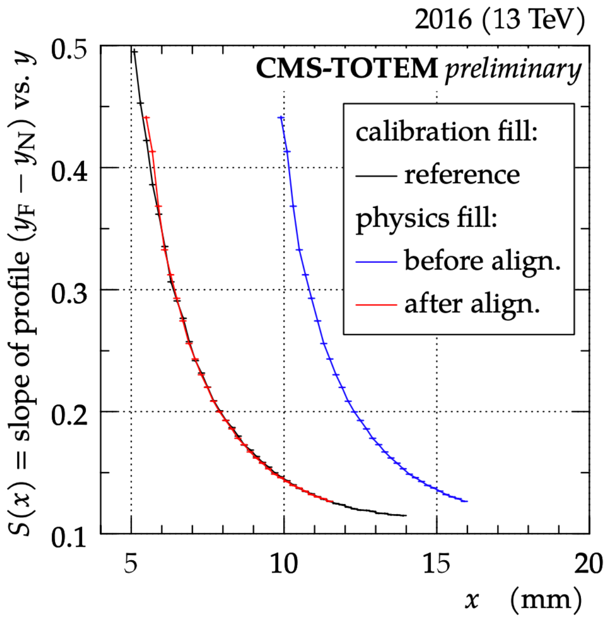

For each high luminosity physics fill, the RPs alignment is obtained by matching observables from the fill to those from the "alignment run" (same optics required!)

Timing RPs are then aligned w.r.t. the tracking RPs

LHC optics: proton transport from IP to PPS

The transport matrix parametrising the LHC magnet lattice relates the transverse position and direction of a proton track along the beam line to the proton kinematics at the IP:

$$\vec{d}(s) = T(s,\xi) \cdot \vec{d}^{*}$$

at IP

$$T = \begin{pmatrix} v_x & L_x & m_{13} & m_{14} & D_x \\ \frac{\mathrm{d}v_x}{\mathrm{d}s} & \frac{\mathrm{d}L_x}{\mathrm{d}s} & m_{23} & m_{24} & \frac{\mathrm{d}D_x}{\mathrm{d}s} \\ m_{31} & m_{32} & v_y & L_y & D_y \\ m_{41} & m_{42} & \frac{\mathrm{d}v_y}{\mathrm{d}s} & \frac{\mathrm{d}L_y}{\mathrm{d}s} & \frac{\mathrm{d}D_y}{\mathrm{d}s} \\ 0 & 0 & 0 & 0 & 1 \end{pmatrix}$$

Transport matrix

Proton transverse positions

$$\vec{d} = (x, \theta_x, y, \theta_y, \xi)^T$$

Proton angles

Proton Δp/p: fractional momentum loss

The reconstruction of the proton kinematics requires the inversion of the transport matrix

A simplified version of the inversion equations, keeping only significant terms:

$$x = v_x(\xi) \cdot x^{*} + L_x(\xi) \cdot \theta_x^{*} + D_x(\xi) \cdot \xi$$
$$y = v_y(\xi) \cdot y^{*} + L_y(\xi) \cdot \theta_y^{*} + D_y(\xi) \cdot \xi$$

Magnification functions

Effective lengths

Dispersions

Optics calibration

Very good knowledge of the LHC beam optics is needed in order to correctly reconstruct the proton fractional momentum loss ξ

- Significant data-driven corrections need to be made to the nominal optics
  - MADX software is used to simulate LHC optics
  - Effective lengths are calibrated using constraints from data and calculated at each detector station
- The horizontal dispersion is calibrated by using the pinch point at $x = x_0$ where $L_y(\xi_0) = 0$: $D_x = x_0 / \xi_0$

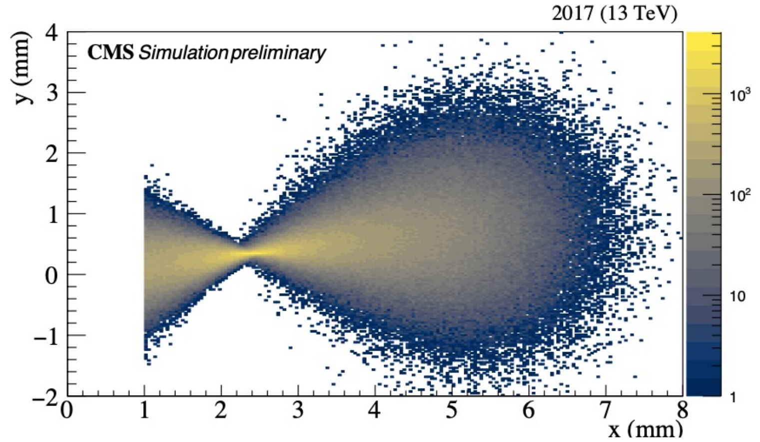

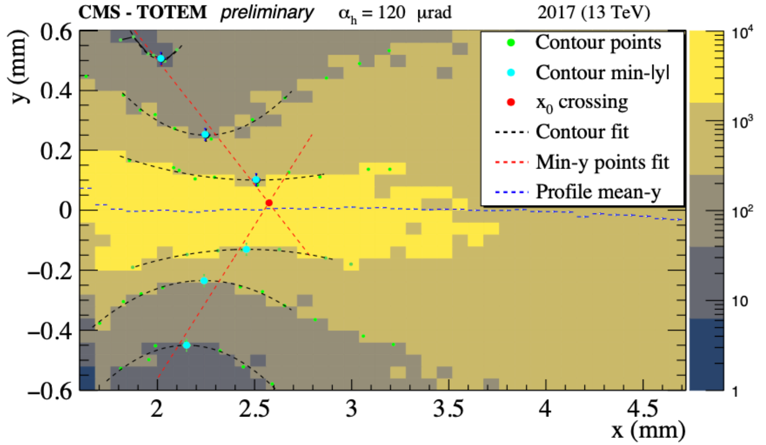

Non-linear calibration of ξ vs. the measured track positions

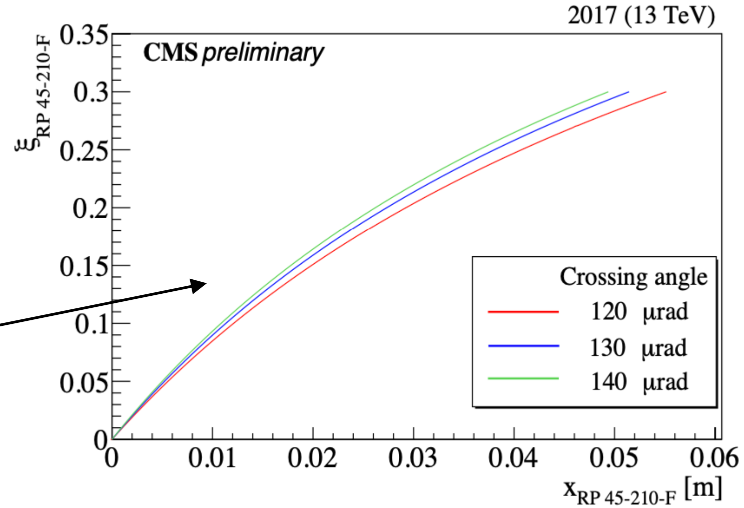

x-to-ξ curves

An interpolation among different crossing angles is performed

Proton kinematics reconstruction

The proton kinematics at the IP are obtained from the measured track positions at the RPs by **back-propagating the proton from the RPs to the IP according to the LHC optics:**

$$x = v_x(\xi) \cdot x^* + L_x(\xi) \cdot \theta_x^* + D_x(\xi) \cdot \xi$$
$$y = v_y(\xi) \cdot y^* + L_y(\xi) \cdot \theta_y^* + D_y(\xi) \cdot \xi$$

Single-RP method:

- Information from a single RP
- Only ξ is reconstructed from x measured in the RP, using the x-to-ξ curves
- Reconstruction neglects impact of horizontal scattering angle -> **limited resolution σ(ξ)**
- **Less sensitivity to systematic uncertainties**

Multi-RP method:

- Combines measurements of RPs in one sector to disentangle ξ and θ^*_x
- Minimization of

$$\chi^2 = \sum_{q=x_N, y_N, x_F, y_F} \left(\frac{q - O_q(x^*, \theta_x^*, y^*, \theta_y^*, \xi)}{\sigma(q)} \right)^2$$

- O_q: optics prediction for the coordinate, given the proton kinematics
- 4 measurements available -> by default x^* is fixed to 0
- Non linearities considered in functions O_q -> **significant improvement in σ(ξ)**
- Assumes careful calibration -> **more complex systematic uncertainty model**

Control plots and acceptance

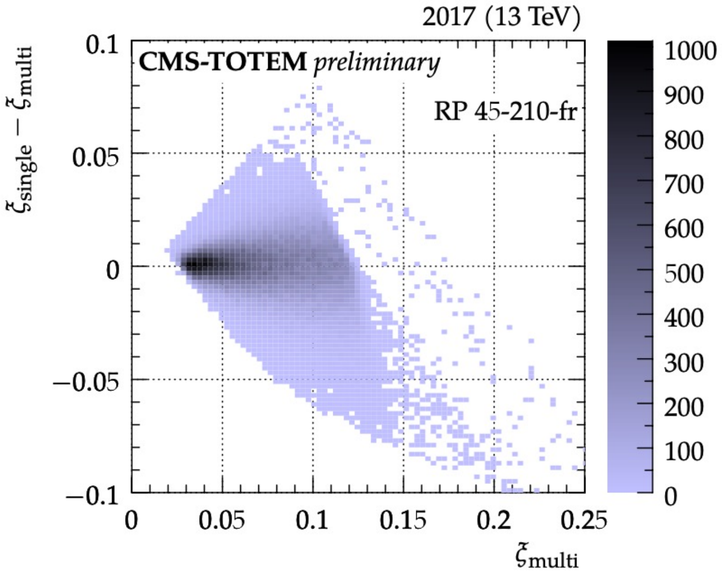

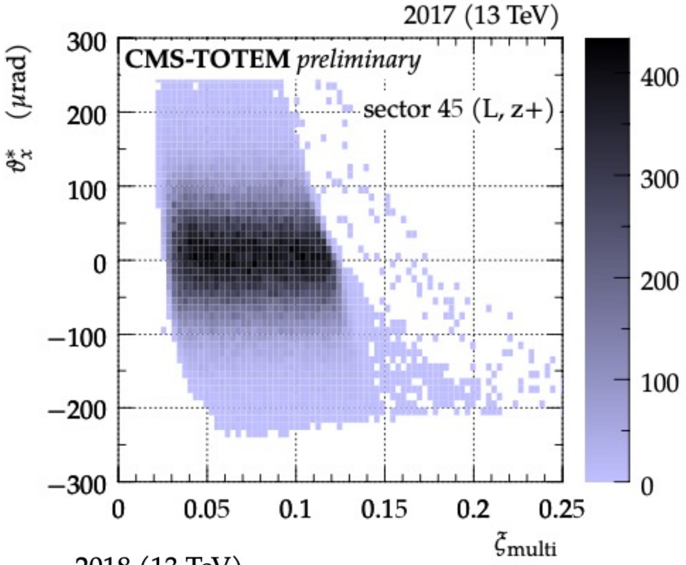

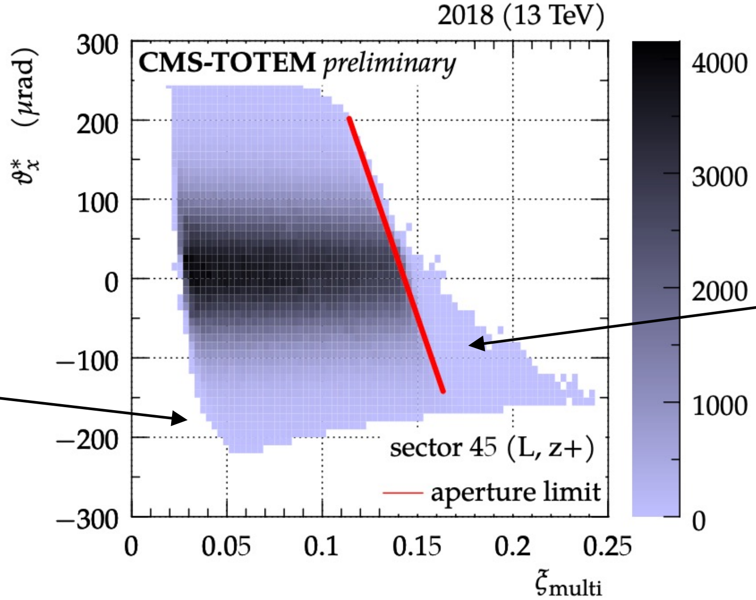

Distance from the beam

LHC aperture limitations, roughly linear dependence on the crossing angle

Proton reconstruction

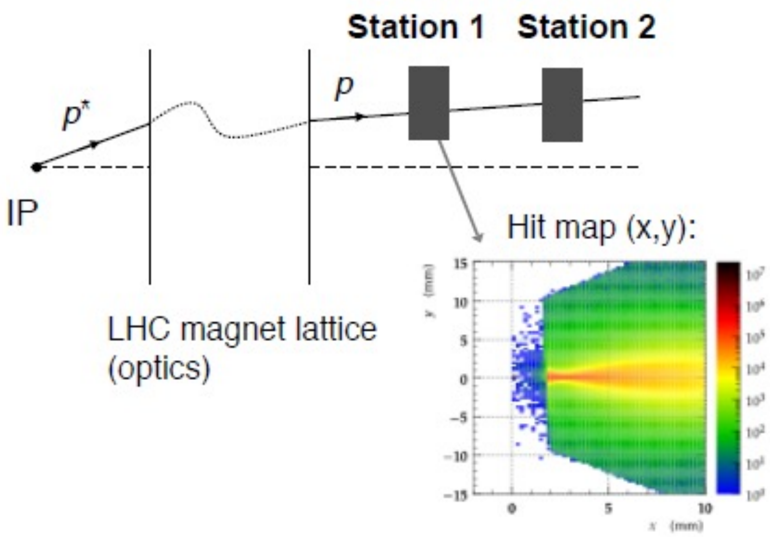

Knowledge of the beam optics allows the proton fractional momentum loss ξ to be computed, from which the invariant mass and the rapidity of the centrally produced state X are determined

$$\xi = 1 - \frac{|p_f|}{|p_i|} \qquad M_X = \sqrt{s\xi_1\xi_2} \qquad y_x = \frac{1}{2}\log\left(\frac{\xi_1}{\xi_2}\right)$$

Double arm mass acceptance in the ~400-2000 GeV range:

- lower limit mainly due to the minimum distance from the beam (may vary depending on beam conditions, e.g. crossing angle)
- upper limit due to collimators

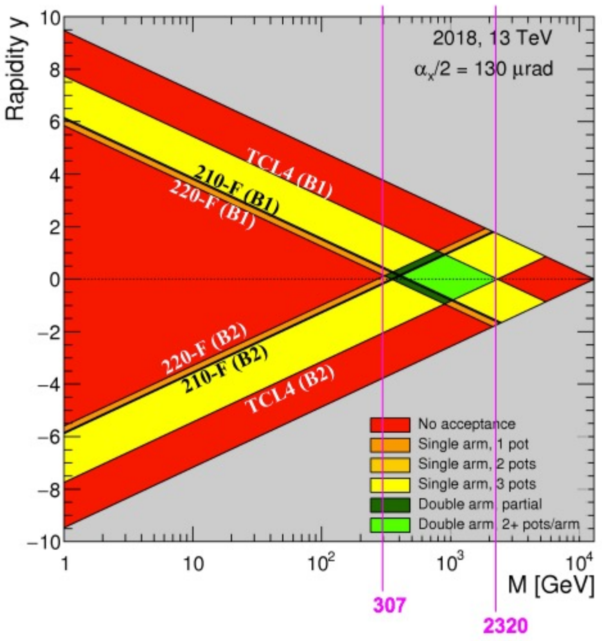

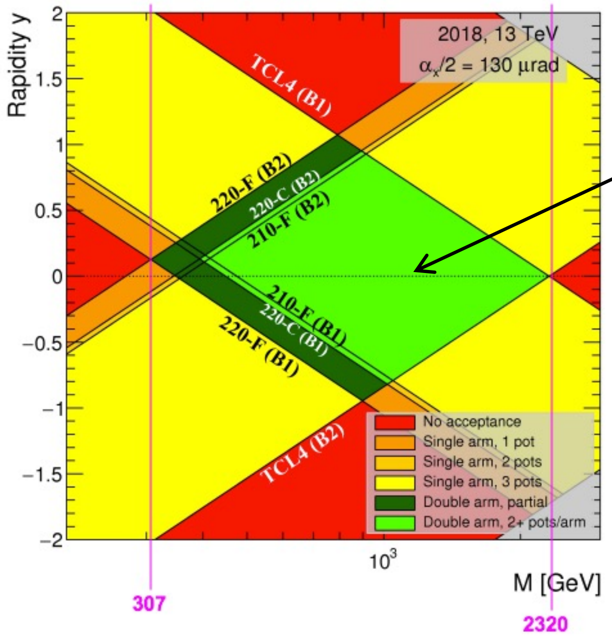

Double arm region

2018 RP acceptance

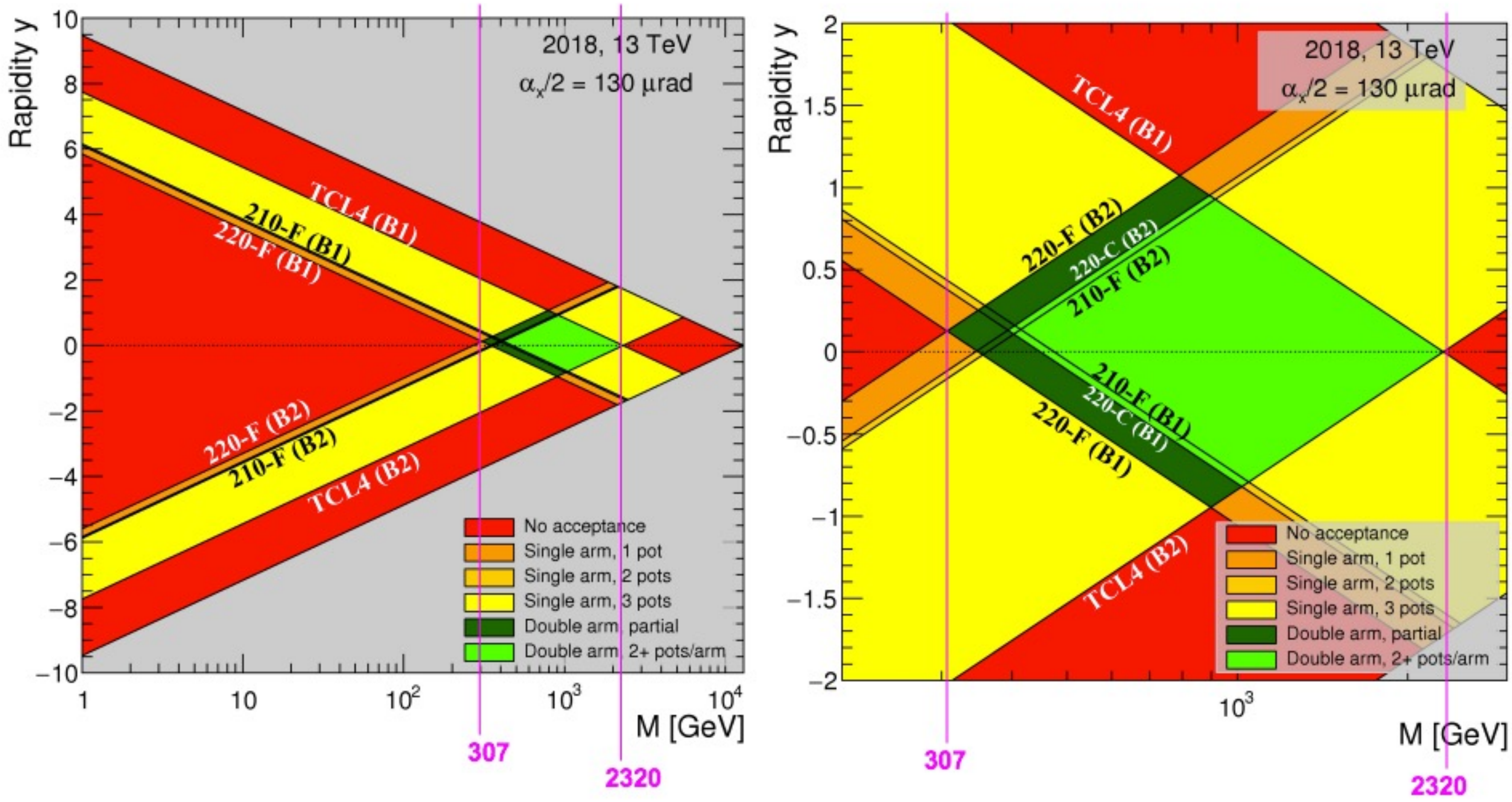

Resolution and systematics studies

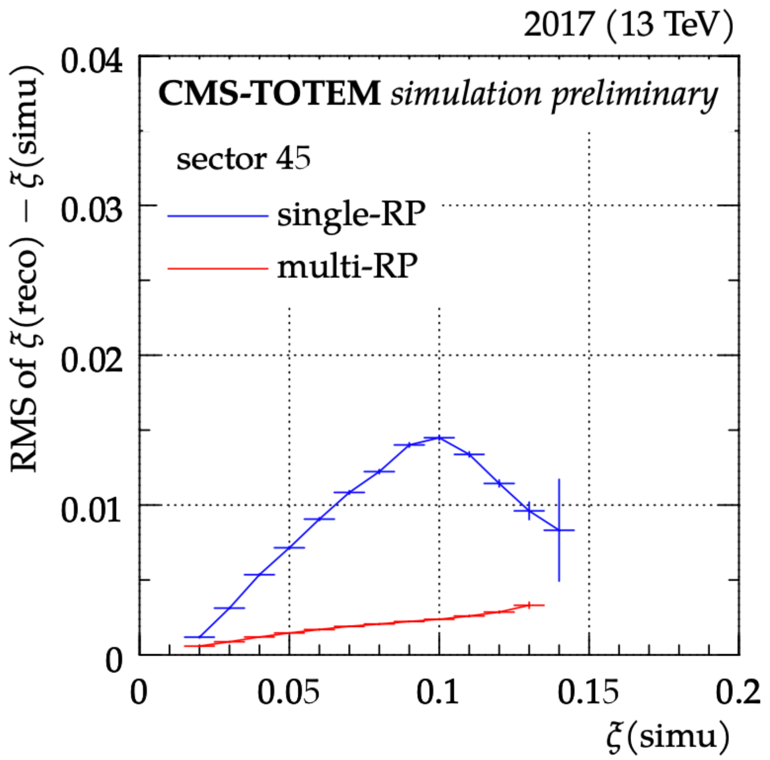

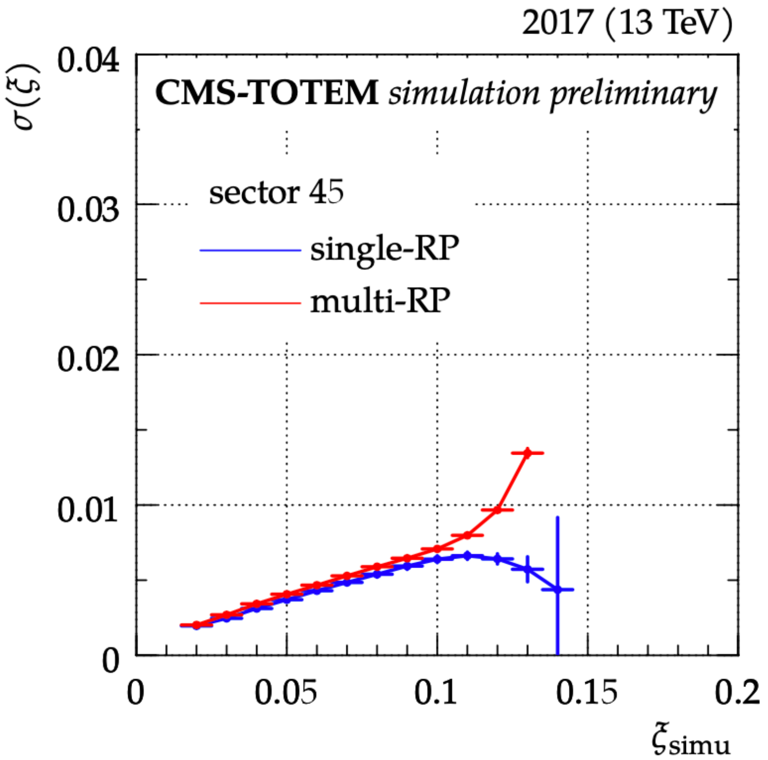

- Single-RP reconstruction resolution dominated by neglecting θ^*_x (at high ξ , width of θ^*_x reduced by LHC collimators)
- Multi-RP reconstruction resolution dominated by detector spatial resolution

- The combination of all studied scenarios is shown, dominated by the uncertainty of the horizontal dispersion
- The change of behaviour at large ξ is due to the LHC collimators
- The multi-RP reconstruction is more sensitive to systematic errors

Proton simulation – validation

Comparison of hit distributions

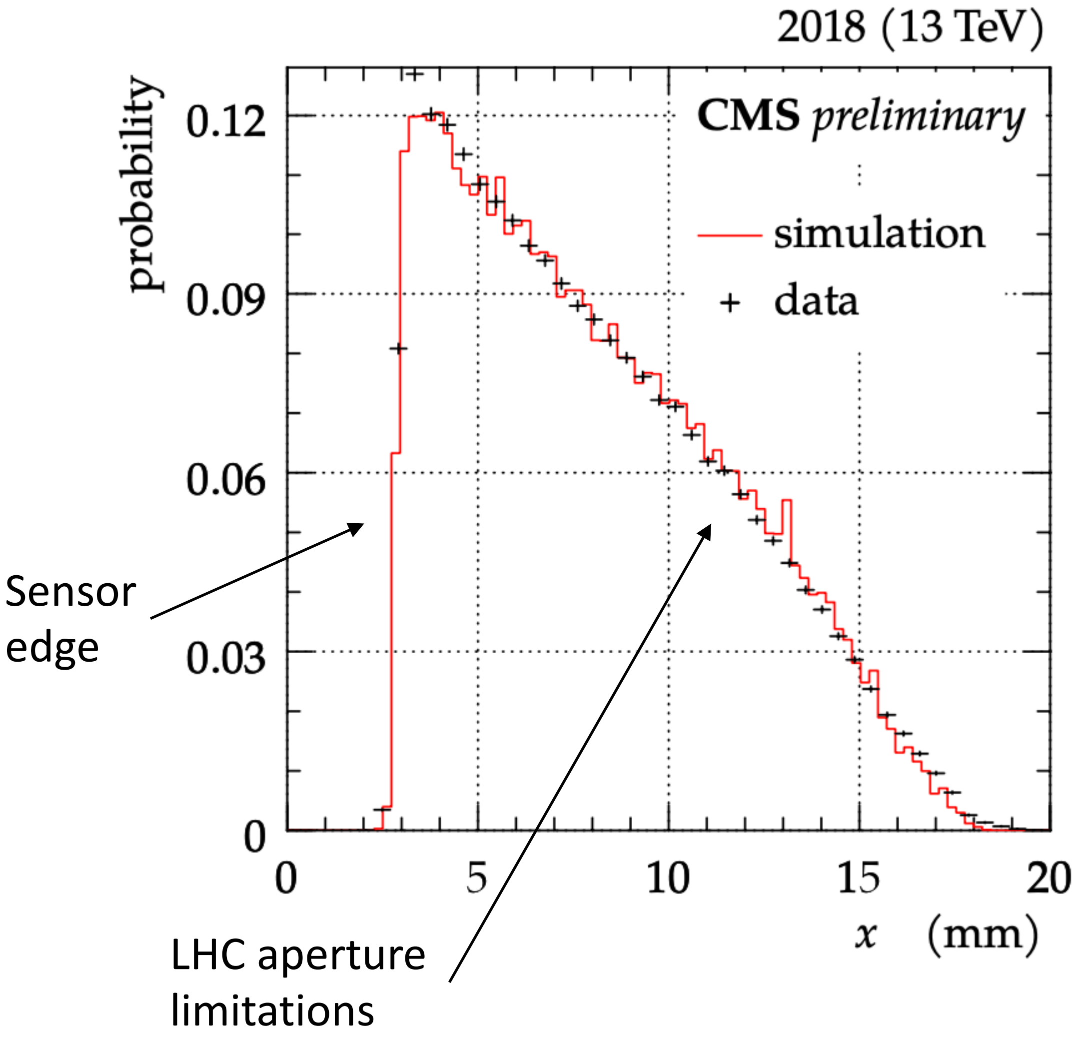

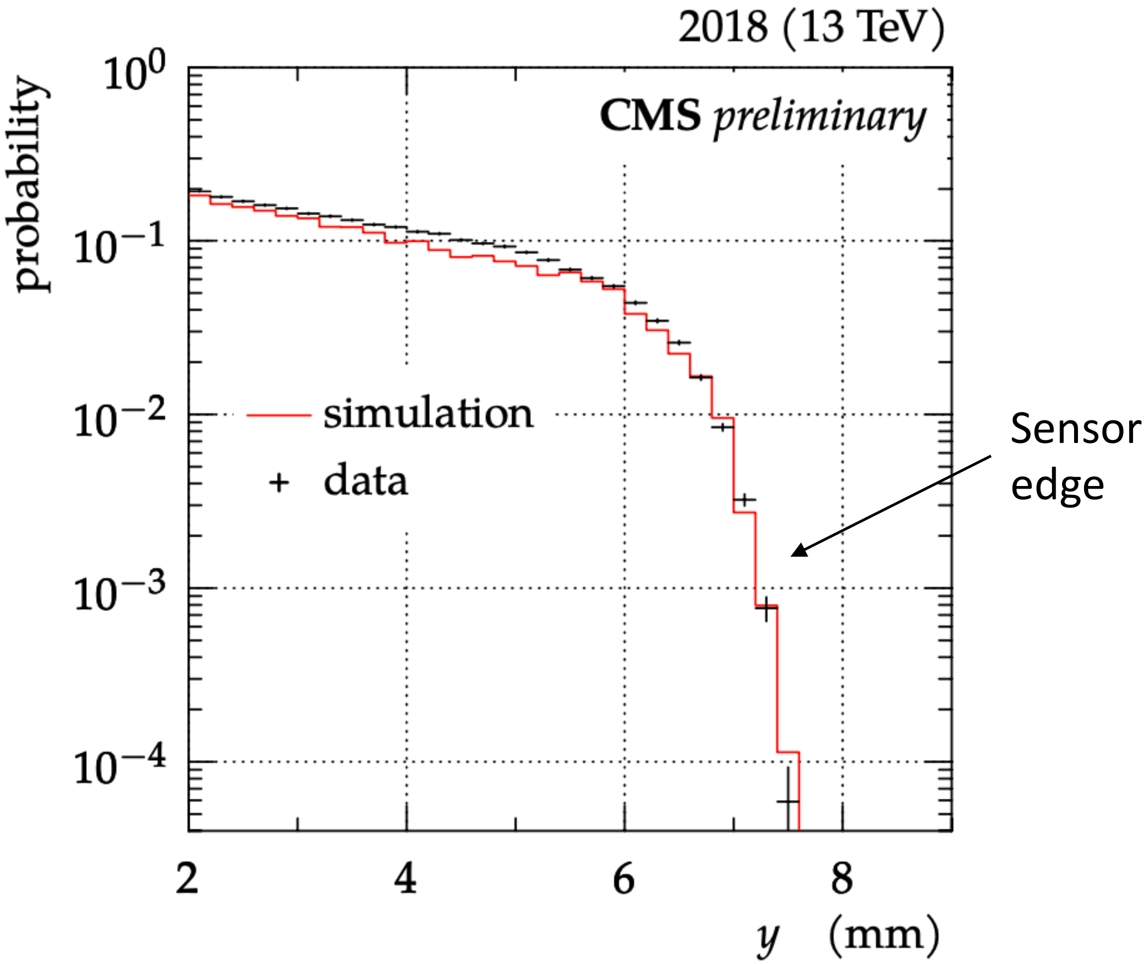

Validation with dimuon control sample (2017-2018)

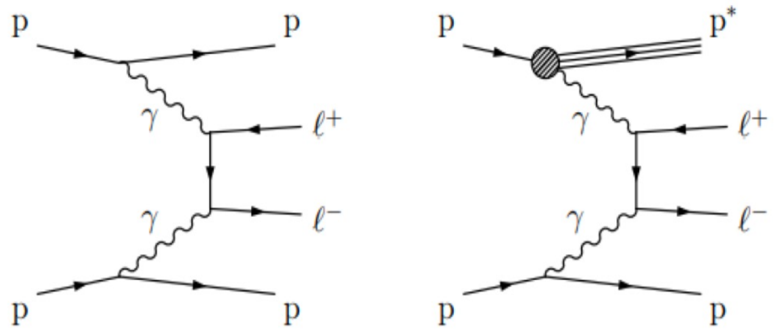

Dilepton analysis with 2017+2018 data, 92.3 fb^{-1}

Correlations between fractional momentum loss reconstructed from dimuon pair ξ(μμ) vs that measured with proton(s) ξ(p) in data
Signal on the diagonal as expected

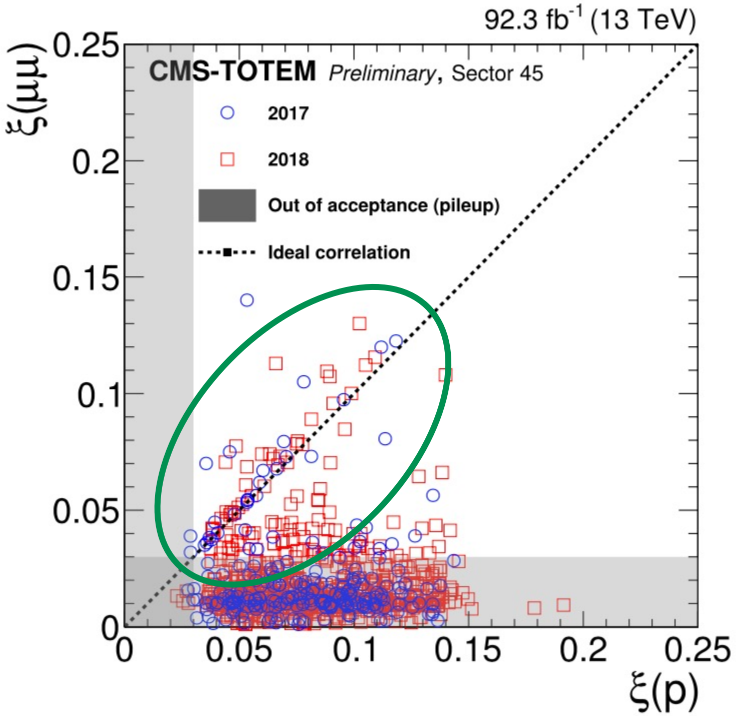

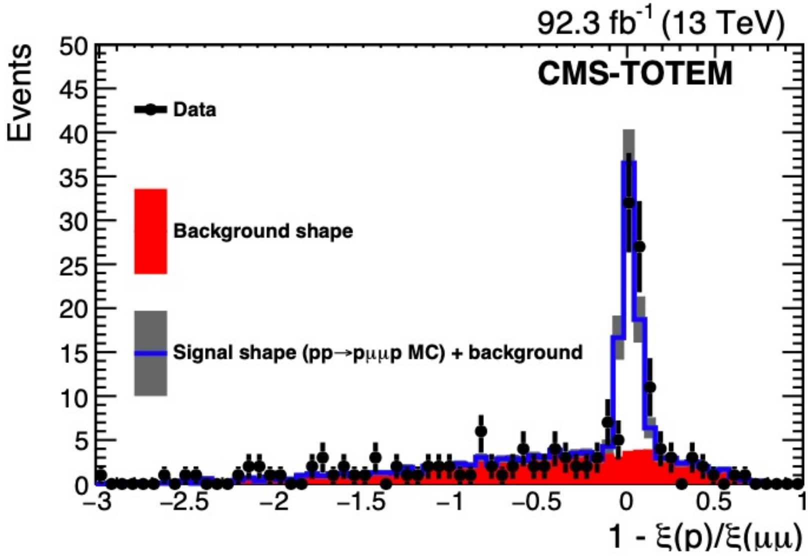

Correlation peak width consistent between data and simulation: **well described resolution**
Peak position at 0 as expected